Hydrodynamic feedbacks of salt-marsh loss in shallow microtidal back-barrier systems

Alvise Finotello[1,2,3*,±], Davide Tognin[2,4,*,±], Luca Carniello[2,4], Massimiliano Ghinassi[1,2], Enrico Bertuzzo[3], Andrea D'Alpaos[1,2]

[1] *University of Padova, Dept. of Geosciences, IT-35131, Padova, Italy.*

[2] *University of Padova, Center for Lagoon Hydrodynamics and Morphodynamics (C.I.Mo.La.), IT-35131, Padova, Italy.*

[3] *Ca' Foscari University of Venice, Department of Environmental Sciences, Informatics and Statistics, IT-30172, Mestre, Venice, Italy.*

[4] *University of Padova, Dept. of Civil, Environmental, and Architectural Engineering, IT-35131, Padova, Italy.*

*Corresponding authors:
Alvise Finotello (`alvise.finotello@unipd.it`)
Davide Tognin (`davide.tognin@phd.unipd.it`)

[±] *these authors contributed equally to this work*

Key Points:

- Past and future feedbacks between salt-marsh loss and back-barrier hydrodynamics are investigated in the microtidal Venice Lagoon
- Marsh disappearance affects the lagoon hydrodynamics both directly and indirectly through cascade effects due to morphodynamic feedbacks
- Hydrodynamic changes depend on site-specific morphological and ecological features of the back-barrier system, as well as on local climate

Keywords

morphodynamics, salt marshes, salt-marsh erosion, back-barrier system, Venice Lagoon

Abstract

Loss of salt marshes in back-barrier tidal embayments has been widely documented worldwide as a consequence of land-use changes, wave-driven lateral erosion of marsh margins, and relative sea-level rise compound by mineral sediment starvation. However, how salt-marsh loss affects the hydrodynamics of back-barrier systems and feeds back into their morphodynamic evolution is still poorly understood. Here we use a custom-built, depth-averaged hydrodynamic model to investigate the mutual feedbacks between salt-marsh erosion and hydrodynamic changes in the Venice Lagoon, a large microtidal back-barrier system facing the Adriatic Sea in north-eastern Italy. Numerical simulations were carried out for past morphological configurations of the lagoon dating back up to 1887, as well as for hypothetical scenarios involving additional marsh erosion

relative to the present-day conditions. We demonstrate that the progressive loss of salt marshes significantly impacted the Venice Lagoon hydrodynamics, both directly and indirectly, by amplifying high-tide water levels, promoting the formation of higher and more powerful wind waves, and critically affecting tidal asymmetries across the lagoon. We also argue that further losses of salt-marsh area would likely have detrimental effects on the lagoon ecomorphodynamic evolution, though with negligible impacts in terms of increased flooding risk in lagoonal urban settlements. Compared to previous studies, our analyses suggest that the hydrodynamic response of back-barrier systems to salt-marsh erosion is extremely site-specific, as it depends closely on the morphological characteristics of the embayment as well as on the external climatic forcings.

1 Introduction

Tidal back-barrier lagoons represent critical environments at the interface between terrestrial, freshwater, and marine habitats (Flemming, 2012; Levin et al., 2001; Pérez-Ruzafa et al., 2019; G. M. E. Perillo, 1995), and are especially common along the World's coasts (Boothroyd et al., 1985; FitzGerald & Hughes, 2019; Kennish, 2016; Stutz & Pilkey, 2011). They consist of sheltered embayments separated from the ocean by a system of barrier islands (Hesp, 2016) interrupted by tidal inlets (De Swart & Zimmerman, 2009), the latter allowing for the exchange of tides, sediments, nutrients, and biota between the back-barrier environment and the open sea (Boothroyd et al., 1985; Carson et al., 1988; Finkelstein & Ferland, 1987; Wei et al., 2022). Back-barrier lagoons provide valuable ecosystem services and support high biodiversity, densely populated urban settlements, and florid economies (Barbier et al., 2011; Costanza et al., 1997; D'Alpaos & D'Alpaos, 2021). However, accelerating sea-level rise, reduced sediment supply to the coasts, enhanced storminess, and increasing anthropogenic pressures exacerbate the threat to back-barrier lagoons and the communities relying on them (Gilby et al., 2021; Passeri et al., 2020). Although the current paradigm indicates that future coastal hazards will be mostly dictated by rising sea levels (Finkelstein & Ferland, 1987; González-Villanueva et al., 2015), previous studies demonstrated how geomorphological changes in tidal embayments, both natural and anthropogenically driven, can feedback into coastal hydrodynamics and ultimately exacerbate, or mitigate, coastal hazards (Carniello et al., 2009; Ferrarin et al., 2015; Pollard et al., 2019; Zhou et al., 2014). Therefore, investigating the feedbacks between ecogeomorphological changes and the hydrodynamic of back-barrier systems is of utmost importance to provide reliable assessments of coastal hazards (Carniello et al., 2009; Donatelli, 2020; Donatelli et al., 2018; Donatelli, Kalra, et al., 2020; Donatelli, Zhang, et al., 2020; Ferrarin et al., 2015; Zarzuelo et al., 2018).

Among the morphological features that characterize shallow tidal embayments, salt marshes are especially common and provide a wide number of precious ecosystem services, including blue-carbon sequestration (Chmura et al., 2003), environmental remediation (Nelson & Zavaleta, 2012), shoreline protection (Möller et al., 2014; Temmerman et al., 2013), and habitat provision (Pennings

& He, 2021; G. M. E. Perillo et al., 2019). The alarming rates of salt-marsh loss observed worldwide (Mcowen et al., 2017; Valiela et al., 2009) have prompted extensive studies on salt-marsh ecomorphodynamics (A. D'Alpaos et al., 2007; Fagherazzi et al., 2012; Finotello, Alpaos, et al., 2022), as well as on the response of these ecosystems to changing hydrodynamic forcings and inorganic sediment supply (A. D'Alpaos et al., 2007; Finotello et al., 2020; FitzGerald & Hughes, 2019; Gourgue et al., 2021; Hughes et al., 2021; Mariotti, 2020; Tommasini et al., 2019). The reverse problem, in contrast, still remains unclear, that is, how salt-marsh loss affects hydrodynamics and the related morphodynamic evolution in shallow coastal bays. This uncertainty is mostly due to the paucity of study cases analyzed so far, thus calling for new insights into the mutual feedbacks between salt-marsh loss and hydrodynamic changes in shallow back-barrier tidal systems (Donatelli, 2020; Donatelli et al., 2018; Donatelli, Zhang, et al., 2020; Silvestri et al., 2018).

Here we aim to fill this knowledge gap by focusing on the microtidal Venice Lagoon (Italy), where extensive marsh losses have been documented over the last two centuries (Carniello et al., 2009; L. D'Alpaos, 2010; Tommasini et al., 2019). We will focus in particular on the feedback between salt-marsh loss and changes in the lagoon's hydrodynamics. We will not account for the loss of biodiversity and ecosystem services that are implicitly associated with marsh disappearance, although these effects are of utmost relevance and should clearly be considered when evaluating the impacts of tidal wetland loss (Barbier et al., 2011; D'Alpaos & D'Alpaos, 2021; Mitsch et al., 2015; Mitsch & Gosselink, 2000; Peter Sheng et al., 2022). The lagoon hydrodynamics will be investigated using a custom-built, depth-averaged numerical model applied to several past morphological configurations of the Lagoon, each reconstructed based on available historical topographic and bathymetric maps. Moreover, exploratory simulations will be performed to unravel the hydrodynamic consequences of additional future losses of salt marshes.

The remainder of the paper is organized as follows. In section 2, we provide a brief overview of the Venice Lagoon and describe in detail the morphological changes, both natural and manmade, observed during the last 130 years. We then outline (Section 3) the main features of the hydrodynamic, wind-wave numerical models employed in this study, together with a description of the computational grids and model forcings used. Section 4 reports the results of the numerical simulations, which are then discussed in detail in Section 5. Concluding remarks (Section 6) close the paper.

2 Geomorphological Setting

Located in the northern Adriatic Sea, and characterized by an area of 550 km^2, the Venice Lagoon is the largest brackish waterbody in the Mediterranean Basin. The Lagoon formed over the last 7500 years covering alluvial Late Pleistocene, silty-clayey deposits locally known as *Caranto* (Zecchin et al., 2008). Its present-day morphology is characterized by the presence of three inlets, namely, from North to South: Lido, Malamocco, and Chioggia (**Figure 1**A-D). Tides follow

a semidiurnal microtidal regime, with a mean spring tidal range of 1 m and maximum tidal oscillations of about 0.75 m around Mean Sea Level (MSL) (e.g., D'Alpaos et al. 2013; Valle-Levinson et al. 2021). Meteorological surges often overlap astronomical tides, thus producing significantly high (low) tides when atmospheric pressure is low (high). In addition, wind-related processes are critical for both the hydrodynamics and morphodynamics of the lagoon, with seasonal wind-storm events exerting a prominent control on the medium- to long-term morphodynamic evolution, that is from decadal to centenary timescales (see e.g., Carniello et al. 2009, 2012).

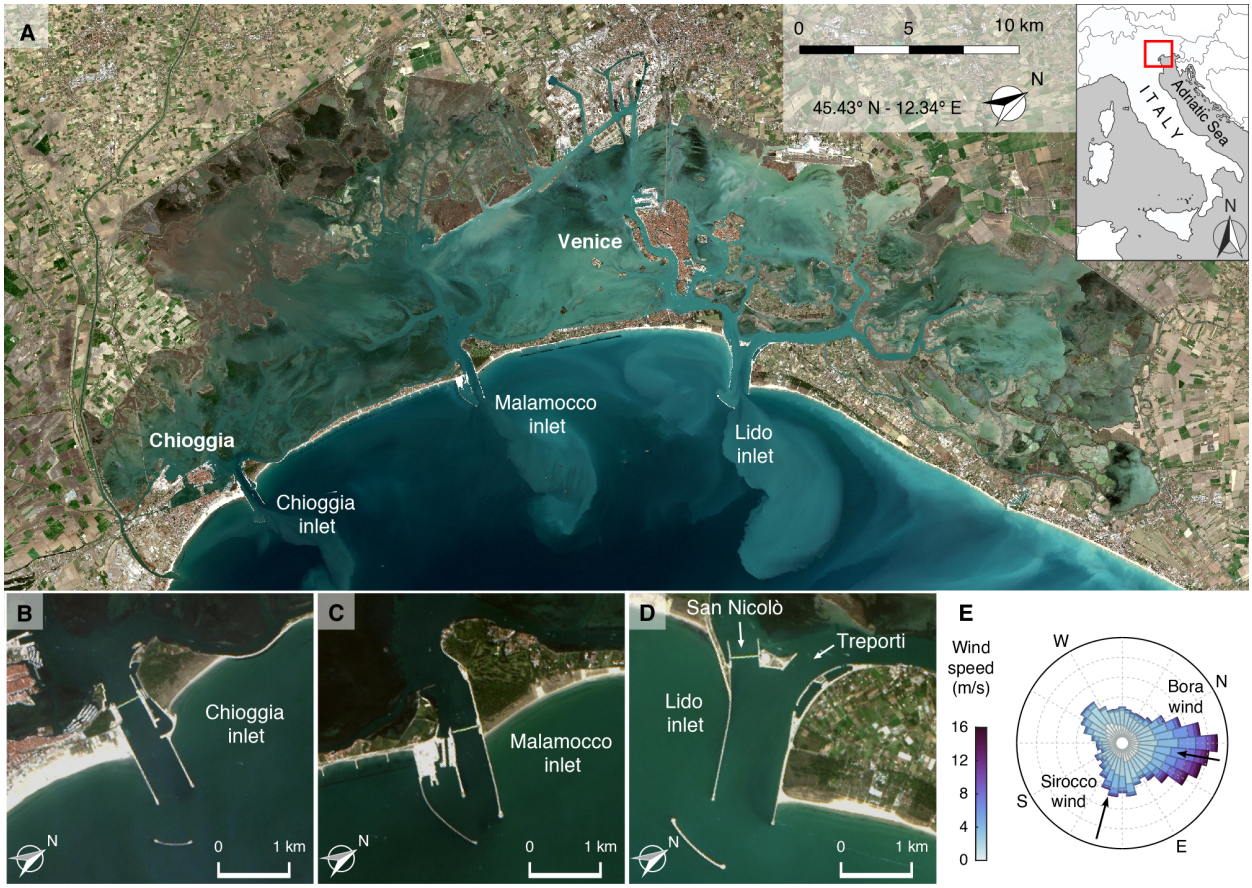

Figure 1: Geomorphological setting. (A) Satellite images of the Venice Lagoon (image ©Google, Landsat). (B,C,D) Close-up views of the three lagoon inlets. (E) Rose-diagram representation of wind climate recorded at the "Chioggia Diga Sud" anemometric station during the period 2000-2019. The two most relevant winds, i.e., the north-easterly Bora wind and south-easterly Sirocco wind, are also highlighted.

The most morphologically and hydrodynamically meaningful wind-storm events

are those associated with *Bora* and *Sirocco* winds, which are also the prevailing winds in the Gulf of Venice (**Figure 1**E). The north-easterly *Bora* winds blow almost parallel to the major axis of the lagoon, thus producing a pronounced setup in the southern lagoon and generating large waves (significant wave height $H_s > 1$ m), which promote significant resuspension of fine sediments expecially from the tidal flats located in the central-southern lagoon. In contrast, *Sirocco* winds blow from South-East and cause large wind-setups in the northern Adriatic Sea, further enhancing high-tide meteorological surges and often leading to extensive flooding of Venice city and other settlements within the Lagoon.

Over the last centuries, the hydrodynamics of the Lagoon was severely affected by anthropogenic interventions (L. D'Alpaos, 2010; Ferrarin et al., 2015). First, by the end of the 16^{th} century, all the major rivers debouching into the lagoon were diverted into the open sea, thus almost completely eliminating fluvial sediment input. Second, between the 1900s and 1970s, extensive land reclamation projects were carried out, especially along the landward margin of the lagoon, to accommodate industrial, agricultural, and fish farming activities, thus importantly reducing the total area open to the propagation of tides (see **Figure 2**). During the same period, extraction of groundwater and natural gas for industrial purposes caused an acceleration in the local subsidence rates, with anthropogenically-induced subsidence reaching cumulative values ranging between 10 to 14 cm in the Venice-City area (Carbognin et al., 2004; Gatto & Carbognin, 1981; Zanchettin et al., 2021). Moreover, in order to allow for increasingly bigger ships to cruise within the lagoon, two large waterways, namely the Vittorio Emanuele and the Malamocco-Marghera channels (**Figure 2**C,D), were excavated in the central part of the lagoon in 1925 and 1968, respectively. Finally, massive jetties were built between 1839 and 1934 at the lagoon inlets to maintain water depths suitable for commercial ship traffic (**Figure 2**A-D). The jetties at the Malamocco inlet were constructed between 1839 and 1872, whereas at the Lido inlet the northern jetty was completed in 1887 (see **Figure 2**A), with the southern jetty added later in 1892 (see **Figure 2**B). Finally, the jetties at the Chioggia inlet were built between 1910 and 1934 (**Figure 2**C). On the one hand, the jetties reduced the width of the inlets, thus resulting in considerable deepening as foreseen during the design phase (**Figure 2**A-C). On the other hand, they caused important changes in the lagoon hydro- and morpho-dynamic regimes. Since the construction of the jetties, changes in the tidal regime within the lagoon have been much more sustained than the typical periodic, multi-annual variations induced by the nodal modulation of tides in the Adriatic Sea, which are in the order of 4% of the characteristic tidal range (Amos et al., 2010; Valle-Levinson et al., 2021). Between 1909 and 1973, the tidal range within the lagoon increased as much as 25% on average (L. D'Alpaos, 2010; Ferrarin et al., 2015; Tomasin, 1974), with local changes that can be even more pronounced (Finotello et al., 2019; Finotello, Capperucci, et al., 2022; Silvestri et al., 2018).

All these interventions, coupled with eustatic sea-level rise (average value 1.23 ± 0.13 mm/year between 1872 and 2019; 2.76 ± 1.75 mm/year between

1993 and 2019; see Zanchettin et al. 2021), had important impacts on the lagoon morphological evolution, triggering positive morphodynamic feedbacks. Progressively larger portions of the lagoon became ebb-dominated, especially close to the inlets where the jetties produced strong ebb-flow asymmetries, enhancing the export of fine sediments and preventing the import of sediment carried in suspension by longshore currents (L. D'Alpaos, 2010). This condition, worsened by anthropogenically-induced starvation of fluvial sediment supply, set a negative sediment budget and resulted in a progressive, generalized loss of salt marshes (Carniello et al., 2009; L. D'Alpaos, 2010; Tommasini et al., 2019; see Figure 2A-F,K), the very existence of which is intimately linked to the availability of external sediment supply (e.g., Roner et al. 2021; Willemsen et al. 2021). Reduced marsh coverage lengthened wind fetches, thus favoring the formation of higher, more energetic waves, which further enhanced the erosion of marsh margins (Finotello et al., 2020; Leonardi, Ganju, et al., 2016; Marani et al., 2011; Mariotti & Fagherazzi, 2013), as well as of tidal-flat beds (Carniello et al. 2009; Tommasini et al. 2019; see Figure 2). Deepening of tidal flats (**Figure 2**L), exacerbated by the eustatic rise in sea levels and both natural and anthropogenic-induced subsidence, promoted the generation of even higher wind waves, which in turn favored additional erosion of salt marshes and tidal flats through a positive feedback loop.

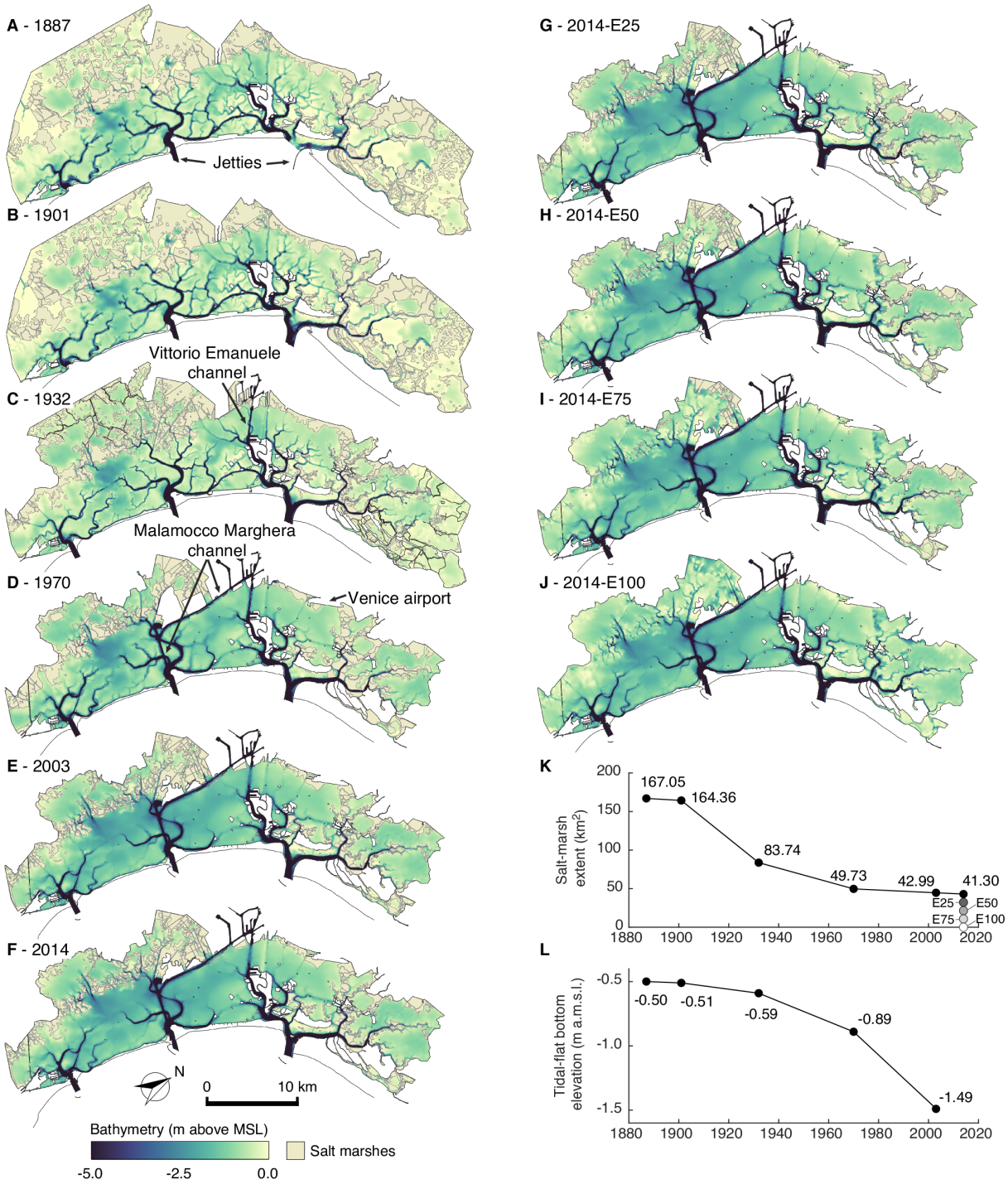
A - 1887
Jetties
B - 1901
Vittorio Emanuele channel
C - 1932
Malamocco Marghera channel
D - 1970
Venice airport
E - 2003
F - 2014
N
0
10 km
Bathymetry (m above MSL)
-5.0
-2.5
0.0
Salt marshes
G - 2014-E25
H - 2014-E50
I - 2014-E75
J - 2014-E100
K
Salt-marsh extent (km²)
200
150
100
50
0
167.05
164.36
83.74
49.73
42.99
41.30
E25
E50
E75
E100
1880
1900
1920
1940
1960
1980
2000
2020
L
Tidal-flat bottom elevation (m a.m.s.l.)
-0.5
-1.0
-1.5
-0.50
-0.51
-0.59
-0.89
-1.49

Figure 2: Morphological evolution of the Venice Lagoon. Bathymetry of the Venice Lagoon in 1887 (A), 1901 (B), 1932 (C), 1970 (D), 2003 (E), and 2014 (F), as reconstructed from available historical topographic and bathymetric data. G,H,I,J) Morphology of the Venice Lagoon according to the hypothetical scenarios of marsh erosion analyzed in the present study. These scenarios assume different rates of marsh erosion equal to 25% (2014-E25), 50% (2014-E50), 75% (2014-E75), and 100% (2014-E100), respectively. Temporal variation of salt-marsh extent (K) and spatially-averaged bottom elevation of tidal flats (L) between 1887 and 2014 are also shown.

Further manmade modifications of the inlet morphologies were carried out between 2006 and 2014 to accommodate the mobile floodgates of the Mo.S.E. ("Modulo Sperimentale Elettromeccanico") system (**Figure 1**B,C,D), designed to protect the city of Venice and other lagoon settlements from extensive floodings (Mel, Viero, et al., 2021). These interventions slightly increased hydraulic resistances and led to both a reduction of tidal amplitude and an increase in tidal-phase delays within the lagoon (Ghezzo et al., 2010; Matticchio et al., 2017), thus partially mitigating the dominance of ebb-tidal flows (e.g., Finotello et al. 2019). In spite of this, however, salt-marsh erosion within the lagoon is still ongoing, though at reduced rates compared to the last century (**Figure 2**K) (Finotello et al., 2020; Tommasini et al., 2019). Moreover, operations of the Mo.S.E. floodgates will further reduce the resilience of salt marshes to rising relative sea levels by preventing inorganic deposition during storm-surge events which, though episodic, critically contribute to marsh accretion in sediment-starving systems such as the Venice Lagoon (Tognin et al., 2021, 2022).

3 Methods

1.
2.
3.

Numerical model

We employed the bidimensional, depth-averaged, finite element numerical model developed by Carniello et al. (2005, 2011), which is suitable to reproduce the hydrodynamics of shallow tidal basins driven by tidal flows and wind fields. In the following, we report a brief description of the model and refer the reader to Carniello et al. (2011) for further details. The model consists of two coupled modules, namely a hydrodynamic and a wind-wave module, and will be referred to as WWTM (Wind-Wave Tidal Model) hereinafter.

The hydrodynamic model solves the bidimensional, depth-averaged shallow water equations, suitably modified to reproduce wetting and drying processes in very shallow and irregular domains, which read (after Defina 2000):

$$\frac{\partial q_x}{\partial t} + \frac{\partial}{\partial x}\left(\frac{q_x^2}{Y}\right) + \frac{\partial}{\partial y}\left(\frac{q_x q_y}{Y}\right) - \left(\frac{\partial R_{\mathrm{xx}}}{\partial x} + \frac{\partial R_{\mathrm{xy}}}{\partial y}\right) + \frac{\tau_{\mathrm{bx}}}{\rho} - \frac{\tau_{\mathrm{wx}}}{\rho} + gY\frac{\partial H}{\partial x} = 0$$

$$\frac{\partial q_y}{\partial t} + \frac{\partial}{\partial x}\left(\frac{q_x q_y}{Y}\right) + \frac{\partial}{\partial y}\left(\frac{q_y^2}{Y}\right) - \left(\frac{\partial R_{\mathrm{xy}}}{\partial x} + \frac{\partial R_{\mathrm{yy}}}{\partial y}\right) + \frac{\tau_{\mathrm{by}}}{\rho} - \frac{\tau_{\mathrm{wy}}}{\rho} + gY\frac{\partial H}{\partial y} = 0$$

$$\eta\frac{\partial H}{\partial t} + \frac{\partial q_x}{\partial x} + \frac{\partial q_y}{\partial y} = 0$$

where t is time, the x and y subscripts denote the directions of a given variable in a Cartesian reference system, q is the flow rate per unit width, R represents the depth-averaged Reynolds stresses, τ_b is the bottom shear stress produced by tidal currents, τ_w is the wind-induced shear stress at the free surface whose elevation is H, ρ stands for the fluid density, g is the gravitational acceleration, Y is the water volume per unit area ponding the bottom (i.e., the equivalent water depth) and η is the wet fraction of the computational domain which accounts for surface irregularities during the wetting and drying processes (see Defina, 2000, for a detailed description of the hydrodynamic equations). A semi-implicit staggered finite element method based on discontinuous Galerkin's approach is used to solve the governing equations (Defina, 2003). In order to solve the closure of the Reynolds stresses which appear in the momentum equations in the two horizontal directions, a suitable eddy viscosity is as customary introduced and evaluated by means of the Smagorinsky (1963)'s model. The horizontal components of the Reynolds stresses then read

$$R_{\mathrm{xx}} = 2\nu_e\left(\frac{\partial q_x}{\partial x}\right)$$
$$R_{\mathrm{xy}} = \nu_e\left(\frac{\partial q_x}{\partial y} + \frac{\partial q_y}{\partial x}\right)$$

The eddy viscosity ν_e differs from the standard one as it also encloses the contribution from the stresses produced by the subgrid momentum exchange, which is yet difficult to evaluate owing to its dependence on the full three-dimensional morphology of the bottom surface (see Defina, 2000 and D'Alpaos and Defina, 2007 for further details). The hydrodynamic module provides the wind-wave module with water levels and depth-averaged velocities that are employed for calculating wave group celerity and bottom shear stresses (induced by both wind waves and tidal currents), as well as for evaluating the influence of flow depth on wind-wave propagation.

The wind-wave module employs the same computational grid of the hydrodynamic model to solve the wave action conservation equation (Holthuijsen et al., 1989). The latter is simplified by assuming that the direction of wave propagation instantaneously readjusts to match the wind direction (i.e., neglecting

refraction). The module describes the evolution of the wave action density (N_0) in the frequency domain and it reads (Carniello et al., 2011):

$$\frac{\partial N_0}{\partial t} + \frac{\partial}{\partial x} c_{\mathrm{gx}}^{'} N_0 + \frac{\partial}{\partial y} c_{\mathrm{gy}}^{'} N_0 = S_0$$

where $c_{\mathrm{gx}}^{'}$ and $c_{\mathrm{gy}}^{'}$ represent the wave group celerity in the x and y direction, respectively, and are used to approximate the propagation speed of N_0 (Carniello et al., 2005; Holthuijsen et al., 1989), while S_0 represents all the source terms describing the external phenomena contributing to wave energy variations, which can be either positive (wind energy input) or negative (bottom friction, white capping, and depth-induced breaking). Based on the relationship between peak-wave period and local wind speed and water depth (Young & Verhagen, 1996), the model can compute both the spatial and temporal distribution of the wave period. The linear wave theory also allows one to relate the local significant wave height to the horizontal orbital velocity at the bottom and, therefore, to the wind-wave induced bottom shear stress (τ_{ww}). The nonlinear interactions between the latter and the current-induced bottom shear stress τ_b are accounted for through the empirical Soulsby's (1995) formulation, which enhances the value of the bottom shear stress τ_{wc} beyond the mere sum of τ_b and τ_{ww} (see detailed descriptions in Carniello et al. (2005), their equations (26) and (27)). The WWTM has been extensively tested and calibrated against both hydrodynamic and wind-wave field data from the Venice Lagoon (Carniello et al., 2005, 2011; L. D'Alpaos & Defina, 2007; Tognin et al., 2022; Tommasini et al., 2019).

Numerical simulations

3.2.1 Computational Grids Numerical simulations were performed considering ten different morphological configurations of the Venice Lagoon (**Figure 2**). Six of these configurations represent actual past-lagoon morphologies, reconstructed from available topographic and bathymetric data (**Figure 2**A-F), while the additional four configurations consist of hypothetical scenarios characterized by additional marsh loss relative to the present-day lagoon morphology (**Figure 2**G-J). Specifically, to understand how marsh loss affected the hydrodynamics of the Venice Lagoon in the past, we utilized six already existing WWTM computational grids representing the morphological configurations of the lagoon from 1887 to 2014 (Figure 2). The 1887 and 1901 grids were constructed based on "Topographic/hydrographic map of the Venice Lagoon" produced by the Genio Civile of Venezia in 1901, and are identical to each other except for the different morphology of the Lido inlet, where only the northern jetty was present in 1887 while both the jetties were completed in 1901. In contrast, different topographic surveys carried out in 1932, 1970, and 2003 by the Venice Water Authority (Magistrato alle Acque di Venezia) were employed to create the computational grids relative to the years 1932, 1970, 2003, and 2014, respectively (Carniello et al., 2009) (Figure 2A-E). The 2014 computational grid is based

on the most recent, 2003, bathymetric survey and accounts also for the anthropogenic modifications at the three inlets related to the Mo.S.E. system, which were completed in 2014 (Figure 2F). All these grids have been accurately calibrated and utilized in several previous studies (Carniello et al., 2009, 2016; L. D'Alpaos, 2010; Finotello et al., 2019, 2020; Finotello, Capperucci, et al., 2022; Silvestri et al., 2018; Tommasini et al., 2019). Because cell-bed elevations in each computational grid refer to the mean sea level recorded when each survey was performed, and numerical simulations were carried out by forcing the model with tidal waves imposed at the open sea boundary and oscillating around the mean sea level (see next paragraph), historical rises in relative sea level are implicitly accounted for.

In contrast, hydrodynamic effects of additional marsh losses were investigated based on four possible scenarios characterized by different degrees of marsh-area loss equal to 25% (E25, Figure 2G), 50% (E50, Figure 2H), 75% (E75, Figure 2I), and 100% (E100, Figure 2J) relative to the present-day marsh extent (see Donatelli et al. 2018). These scenarios were modeled utilizing the 2014 computational grid as a baseline, and gradually removing marsh areas following the approach adopted by Donatelli et al. (2018). Specifically, computational elements located along eroding marsh margins are selected and their characteristics in terms of elevation and roughness are modified to match those of the surrounding tidal flats. The major shortcoming of this approach is that the hydrodynamic effects of marsh erosion may be largely dependent on the location of the eroded marshes. To overcome this limitation and provide plausible results, marsh elements are removed preferentially where larger wind-induced erosion rates are observed based on combined remote sensing analyses and numerical modeling of wave power (see Tommasini et al. 2019; Finotello et al. 2020). The mean sea level was held constant in all the simulations involving additional loss of salt marsh area. It is worthwhile noting that this approach implicitly assumes that sediments eroded from salt marshes are almost instantaneously removed from the basin, so that they can no longer contribute to active sedimentation on either tidal flats or salt marshes and potentially mitigate the negative effects of marsh loss (Elsey-Quirk et al., 2019; Mariotti & Carr, 2014). Hence, even though our analyses can hardly be used to draw inferences on the long-term effects of marsh loss on the lagoon net sediment budget, they can still be considered representative of possible scenarios of marsh loss in the Venice Lagoon, especially in view of the reduced sediment input to the marshes expected after the activation of the Mo.S.E. barrier system (Tognin et al., 2021).

3.2.2 Boundary Conditions In the numerical model, water levels are imposed at the seaward boundary of the computational domain, the latter including also a portion of the northern Adriatic Sea in front of the Venice Lagoon (see **Figure 3**B). Water level data are measured at the CNR Oceanographic Platform, which is located in the Adriatic Sea, about 15 km away from the coastline. In contrast, data concerning wind speeds and directions are measured at the "Chioggia Diga Sud" anemometric station (**Figure 3**B) and are applied to the

whole lagoonal basin, as they nicely correlate with wind measurements in other locations within the lagoon (see Carniello et al., 2005 for details).

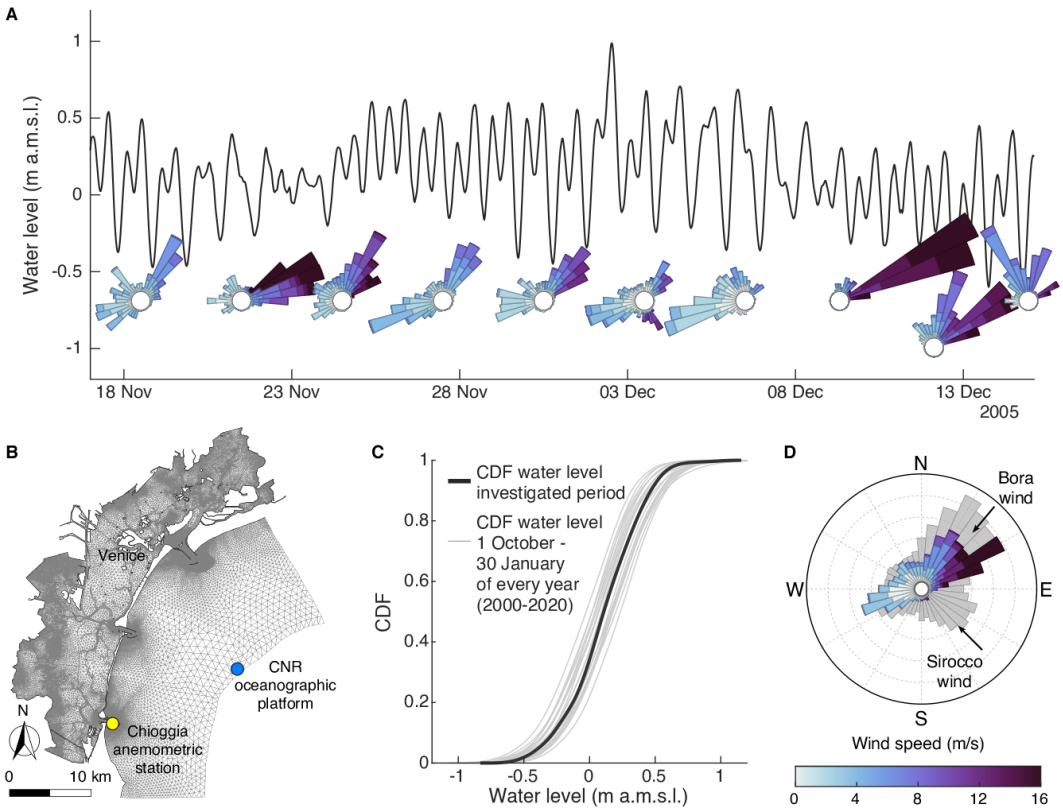

Figure 3: Numerical modeling. (A) Water level and wind climate data utilized for the numerical simulations. Data refer to the period 17 November 2005 – 17 December 2005. Water levels were measured at the "Punta della Salute" tidal-gauge station, whereas wind data were retrieved from the "Chioggia Diga Sud" anemometric station (see panel B). (B) An example of the computational grid employed by the model, referred to the 2014 morphological configuration of the Venice Lagoon. (C,D)Distributions of water levels (C) and wind climate (D) during the analyzed period are compared to those observed over the period 2000-2019 (in grey).

All the simulations were carried out employing the same boundary conditions, thus allowing for a comparison of the effects directly related to morphological changes in the lagoon hydrodynamics. Specifically, the model was forced using hourly water levels and both wind velocities and directions measured from November 16$^{\text{th}}$, 2005 to December 17$^{\text{th}}$, 2005 (**Figure 3**A). The selected 30-day-long study period is representative of hydro-meteorological conditions experienced every year by the Venice Lagoon between October 1$^{\text{st}}$ and January 30$^{\text{th}}$,

which is the period typically characterized by the most significant storm-surge events.

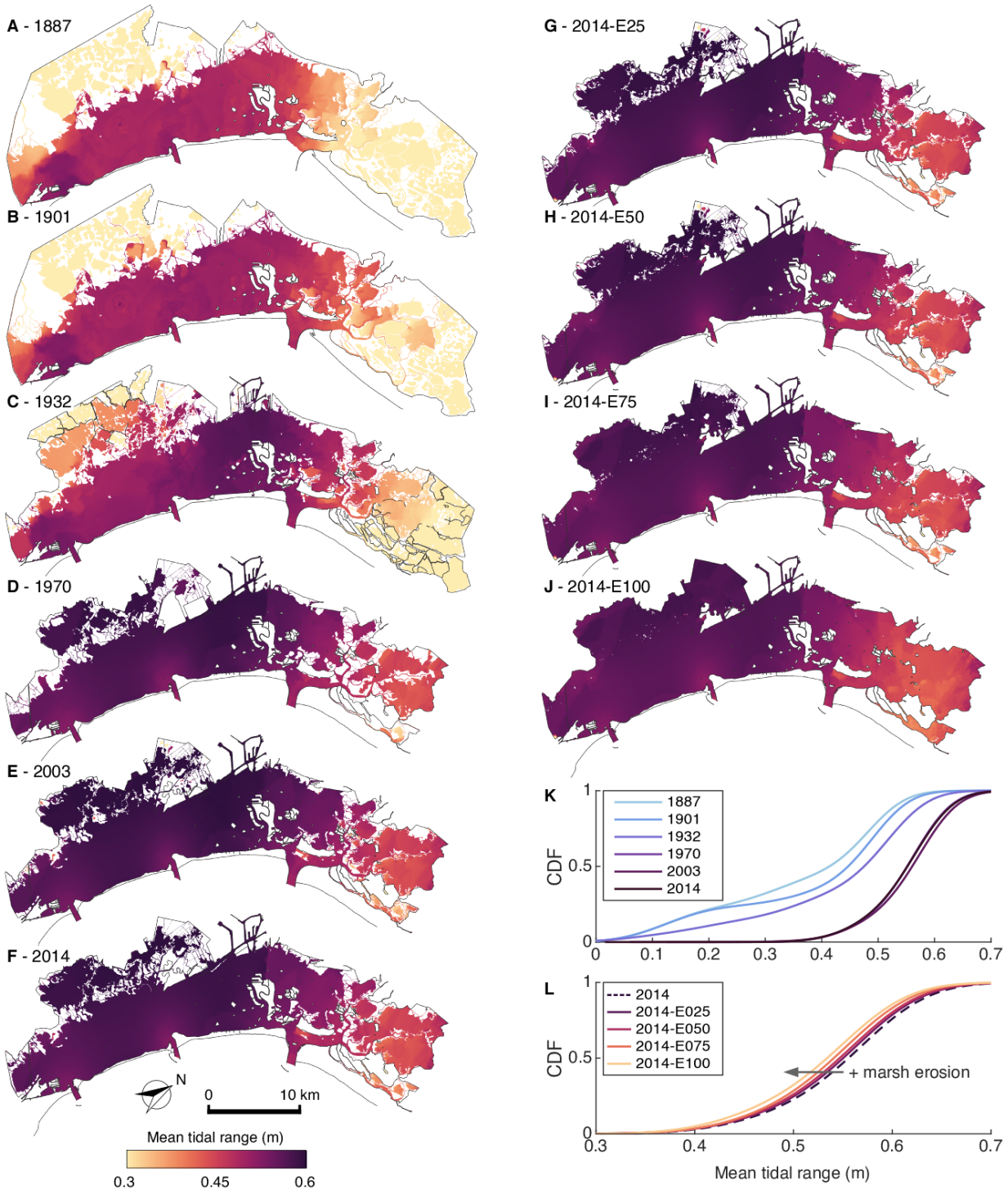
A - 1887
B - 1901
C - 1932
D - 1970
E - 2003
F - 2014
N
0
10 km
Mean tidal range (m)
0.3
0.45
0.6
G - 2014-E25
H - 2014-E50
I - 2014-E75
J - 2014-E100
K
CDF
1887
1901
1932
1970
2003
2014
L
2014
2014-E025
2014-E050
2014-E075
2014-E100
+ marsh erosion
Mean tidal range (m)

Figure 4: Evolution of mean tidal range ($\overline{\Delta h}$). Spatially-explicit representation of $\overline{\Delta h}$ in 1887 (A), 1901 (B), 1932 (C), 1970 (D), 2003 (E), 2014 (F), 2014-E25 (G), 2014-E50 (H), 2014-E75 (I), 2014-E100 (J). (K) Cumulative frequency (CDF) of $\overline{\Delta h}$ for the historical configurations (1887-2014). (L) Cumulative frequency of $\overline{\Delta h}$ in the hypothetical marsh erosion scenarios (2014-E25, E50, E75, E100).

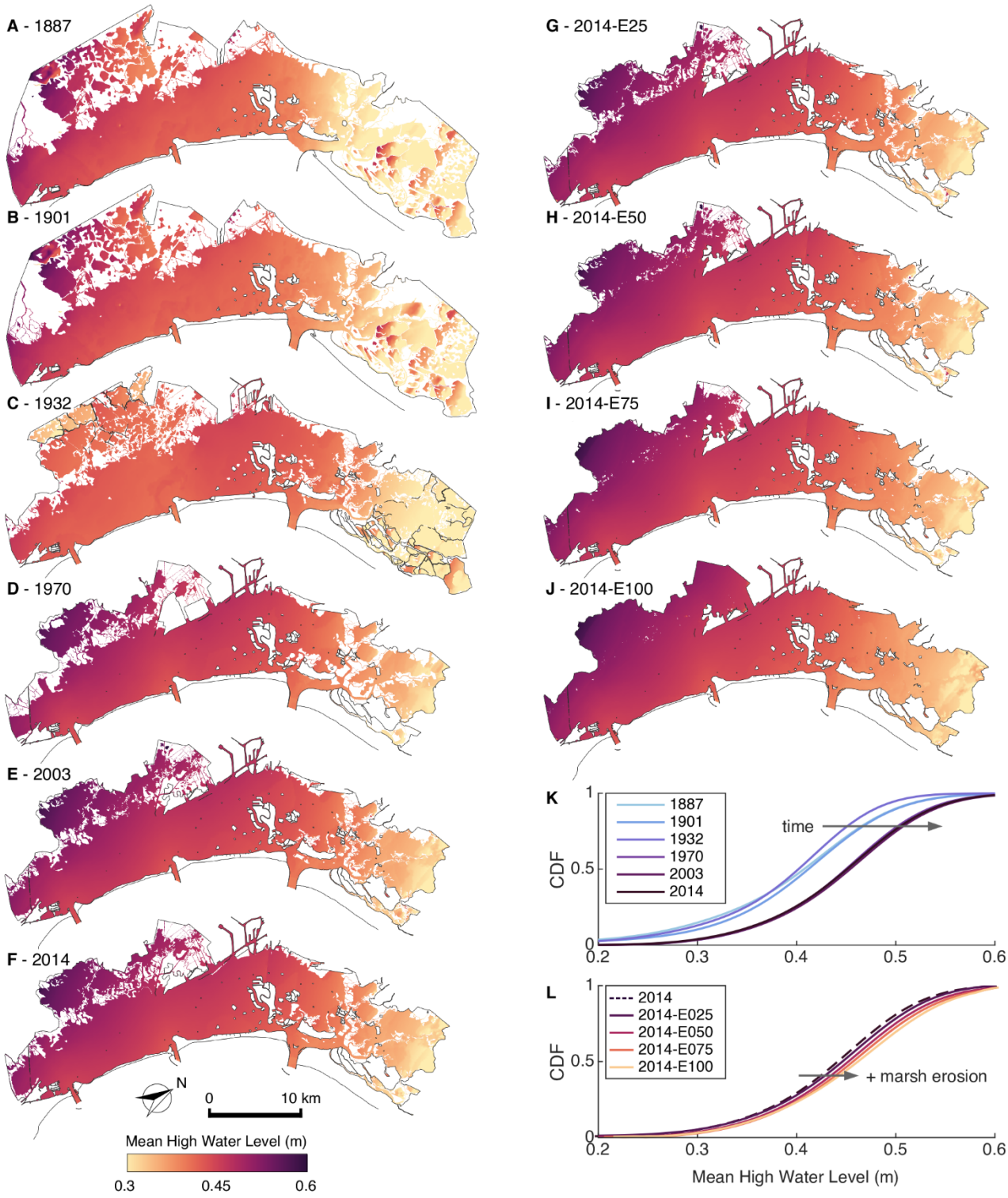
A - 1887
B - 1901
C - 1932
D - 1970
E - 2003
F - 2014
G - 2014-E25
H - 2014-E50
I - 2014-E75
J - 2014-E100
N
0
10 km
Mean High Water Level (m)
0.3
0.45
0.6
K
CDF
1887
1901
1932
1970
2003
2014
time
L
2014
2014-E025
2014-E050
2014-E075
2014-E100
+ marsh erosion
Mean High Water Level (m)

Figure 5: Evolution of mean-high water level (MHWL). Spatially-explicit representation of MHWL in 1887 (A), 1901 (B), 1932 (C), 1970 (D), 2003 (E), 2014 (F), 2014-E25 (G), 2014-E50 (H), 2014-E75 (I), 2014-E100 (J). (K) Cumulative frequency (CDF) of MHWL for the historical configurations (1887-2014). (L) Cumulative frequency of MHWL in the hypothetical marsh erosion scenarios (2014-E25, E50, E75, E100)

.More in detail, the cumulative frequency of water levels for the selected study period is the closest to the average distribution observed between 2000 and 2020 (**Figure 3**C). Moreover, the study period is characterized by two relatively strong Bora wind events (**Figure 3**A) that are typical of the wind climate observed in the Venice Lagoon (**Figure 3**D). Thus, the selected study period allows us to focus both on characteristic tides as well as significant wind-wave events.

The hydrodynamic effects of morphological changes at the whole lagoon scale will be investigated by considering different parameters (e.g., local tidal range, mean high water level, wave height) related to both tides and wind waves. The parameters of interest are computed for each element of the computational grid, and will be presented both in a spatially-explicit fashion as well as in the form of cumulative frequency distributions (CDF) for all the analyzed morphological configurations of the lagoon, to provide a synthetic description of their changes through time and in the four scenarios characterized by different degrees of marsh-area loss assumed as possible future configurations of the lagoon.

4 Results

1.

Water Levels

Concerning water levels within the lagoon, we first focused on the mean tidal range ($\overline{\Delta h}$, **Figure 4**), computed as the average of the local difference Δh between two consecutive high- and low-tide water levels. Overall, results show a continued increase of $\overline{\Delta h}$ from 1887 to 2003, though spatially-explicit representations suggest that such an increase is not spatially homogeneous. Increases in $\overline{\Delta h}$ between 1887 and 1901 are mostly limited to the northern lagoon (**Figure 4**A,B), whereas between 1901 and 1932 enhanced $\overline{\Delta h}$ values are observed especially in the southern lagoon and in the surroundings of Venice City (**Figure 4**B,C). The most pronounced and generalized increase in $\overline{\Delta h}$ is however observed between 1932 and 1970 (**Figure 4**D), as a result of extensive loss of marshlands, the disappearance of many minor branches of tidal channel networks, and generalized tidal-flat deepening (see **Figure 2**D). In contrast, only minor changes are observed from 1970 onwards (**Figure 4**D,E,F), with probability distributions suggesting only a slight increase in $\overline{\Delta h}$ between 1970 and 2003 followed by a reduction between 2003 and 2014 (**Figure 4**K). Numerical simulations involving additional loss of salt-marsh areas suggest that slight $\overline{\Delta h}$ reductions may occur proportional to the percentage of marsh area being lost

(**Figure 4**L).

Following its definition, the mean tidal range ($\overline{\Delta h}$) can only be used to quantify the mean absolute amplitude of tidal oscillations, whereas it does not embed any information regarding possible changes in high water levels due to modifications of tide propagation as a consequence of morphological changes at the basin scale. Therefore, aiming to better characterize changes in the tidal regime, we also investigated how modifications of the lagoon morphology affected the Mean High Water Level (MHWL). The MHWL is defined as the average of all the water levels maxima observed during the study period and thus it represents a meaningful proxy to estimate changes in flooding risk in urban areas within the lagoon. Overall, a generalized increase in MHWL occurred during the study period (**Figure 5**A-F). A slight attenuation of MHWL is observed between 1901 and 1932 (**Figure 5**K), which is nonetheless followed by a pronounced MHWL increase between 1932 and 1970 (**Figure 5**K), when more than half of the total marsh area was already lost (see **Figure 2**K) and the lagoon underwent significant morphological changes (see **Figure 2**C,D). After 1970, only minor increases in MHWL are observed until 2014 (**Figure 5**K). However, exploratory simulations suggest that progressive, additional loss of salt marshes could result in further MHWL increases relative to the values observed in 2014 (**Figure 5**).

Wind waves and bottom shear stresses

Besides tides, wind waves play a fundamental role in the hydrodynamics and morphodynamics of shallow tidal systems, in general (e.g., Green and Coco 2014), and of the Venice Lagoon, in particular (Carniello et al., 2011). To quantify changes in wind-wave fields through time, we focus here on the maximum significant wave height ($H_{s_{\mathrm{MAX}}}$, **Figure 6**). $H_{s_{\mathrm{MAX}}}$ invariably increases through time in all the considered historical configurations, but only minor changes occurred before 1932 (**Figure 6**A,B,C,K). Conversely, between 1932 and 1970, pronounced increases in $H_{s_{\mathrm{MAX}}}$ are observed, especially in the central and southern portions of the lagoon, which are the areas most exposed to the action of Bora winds (**Figure 6**D). Although after 1970 the distribution of $H_{s_{\mathrm{MAX}}}$ does not display substantial changes until 2014 (Figure 6E,F,K), numerical simulations considering additional loss of salt marshes suggest that $H_{s_{\mathrm{MAX}}}$ will increase further proportionally to the percentage of salt-marsh area being lost (Figure 6G-J and L). The most important increases in $H_{s_{\mathrm{MAX}}}$ are to be expected in areas that are nowadays occupied by extensive salt marshes (**Figure 6**G-J), that is, in the whole northern lagoon as well as the most landward portions of the central-southern lagoon (see **Figure 2**F).

The key role exerted by wind waves on the lagoon morphodynamics is related to their ability to determine sediment resuspension from shallow tidal-flat areas, a process whose intensity depends nonlinearly on the wave characteristics. Specifically, wind waves produce large bottom shear stresses (τ_{ww}), which compound the bottom shear stresses induced by tidal currents (τ_b) and determine the total shear stresses (τ_{wc}) that eventually lead to sediment resuspension when

τ_{wc} exceeds the critical threshold for erosion (Carniello et al. 2012; see section 3.1). Numerical results suggest that within channels, where τ_b is typically dominant, only minor increases in τ_{wc} maxima occurred over time (**Figure 7**A-F). In contrast, across shallow tidal flat areas, where the wave-induced bottom shear stress component (τ_{ww}) is predominant, the maximum values of τ_{wc} invariably increases from 1887 to 2014 (**Figure 7**A-F). This process, which is consistent with changes in maximum wave heights ($H_{s_{MAX}}$), eventually leads to a generalized increase of τ_{wc} across the entire lagoon, especially between 1932 and 1970 (**Figure 7**K). Numerical simulations with additional losses of salt marshes suggest that τ_{wc} maxima will be further enhanced proportionally to the marsh area being lost (**Figure 7**G-J, L), in agreement also with the modelled increase in maximum wave height (**Figure 6**L).

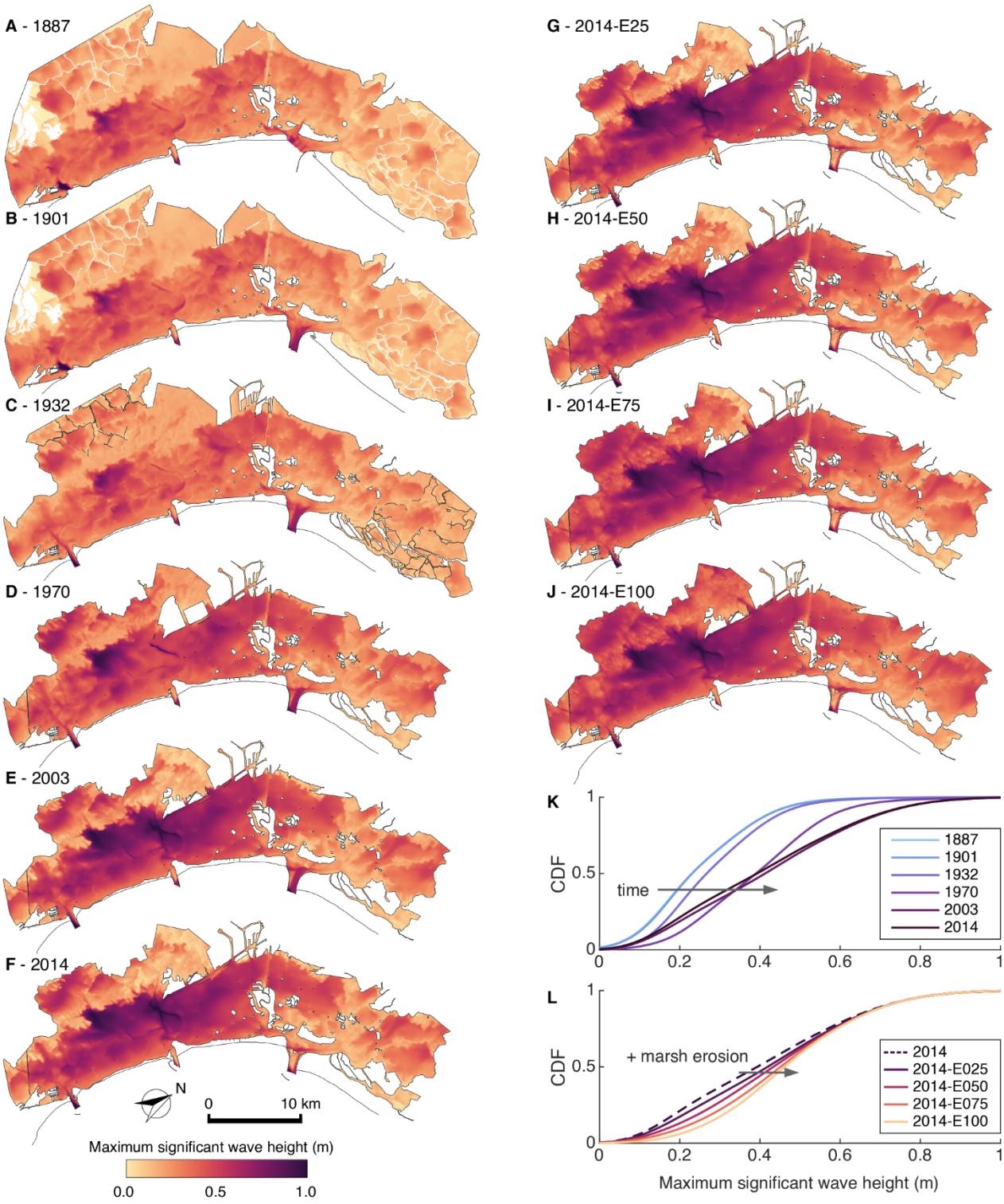
A - 1887
B - 1901
C - 1932
D - 1970
E - 2003
F - 2014
G - 2014-E25
H - 2014-E50
I - 2014-E75
J - 2014-E100
N
0
10 km
Maximum significant wave height (m)
0.0
0.5
1.0
K
CDF
time
1887
1901
1932
1970
2003
2014
L
CDF
+ marsh erosion
2014
2014-E025
2014-E050
2014-E075
2014-E100
Maximum significant wave height (m)

Figure 6 Evolution of maximum significant wave height ($H_{s_{\max}}$). Spatially-explicit representation of $H_{s_{\max}}$ in 1887 (A), 1901 (B), 1932 (C), 1970 (D), 2003 (E), 2014 (F), 2014-E25 (G), 2014-E50 (H), 2014-E75 (I), 2014-E100 (J). (K) Cumulative frequency (CDF) of $H_{s_{\max}}$ for the historical configurations (1887-2014). (L) Cumulative frequency of $H_{s_{\max}}$ in the hypothetical marsh erosion scenarios (2014-E25, E50, E75, E100)

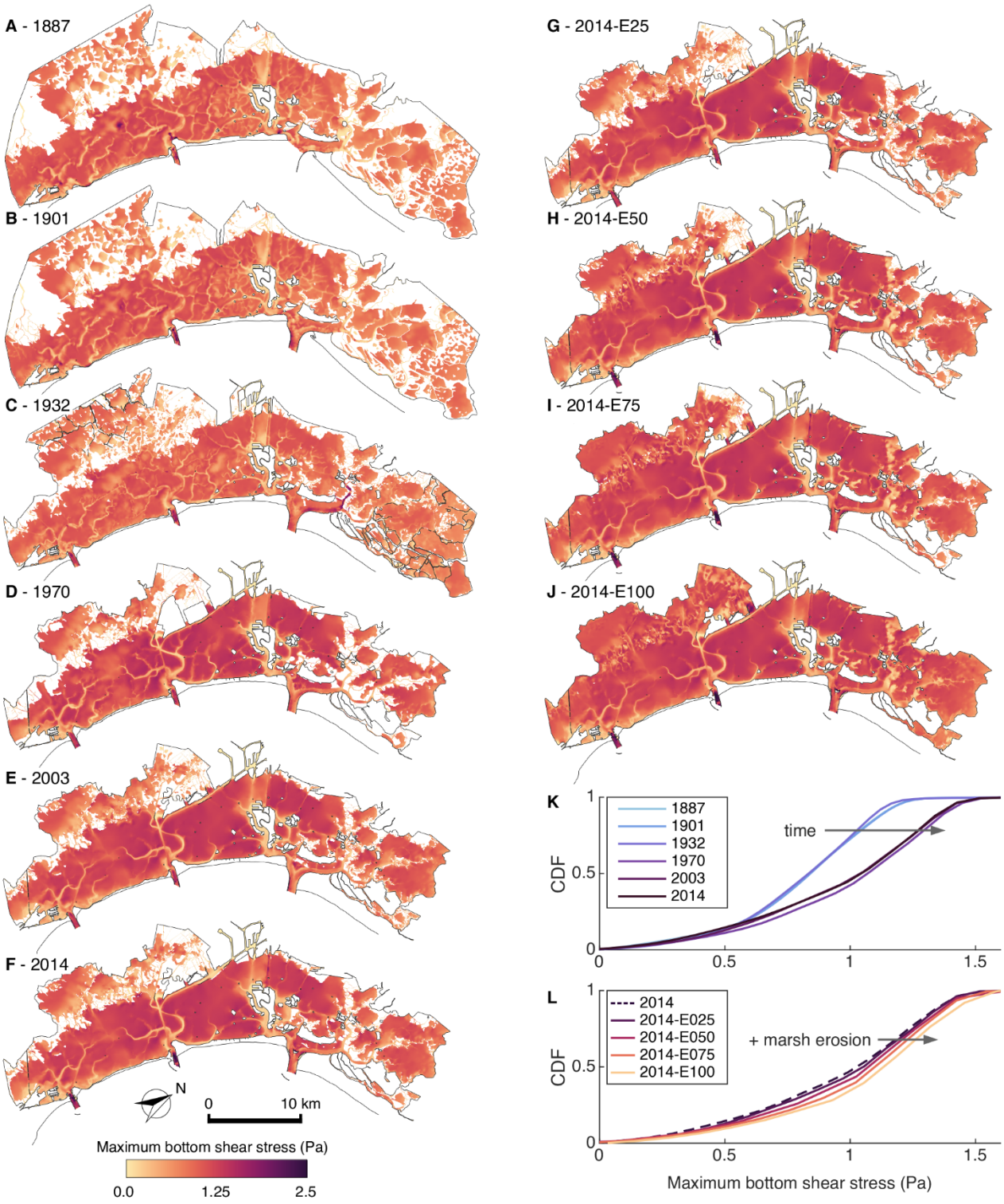
A - 1887
B - 1901
C - 1932
D - 1970
E - 2003
F - 2014
G - 2014-E25
H - 2014-E50
I - 2014-E75
J - 2014-E100
N
0
10 km
Maximum bottom shear stress (Pa)
0.0
1.25
2.5
K
CDF
1887
1901
1932
1970
2003
2014
time
L
2014
2014-E025
2014-E050
2014-E075
2014-E100
+ marsh erosion
Maximum bottom shear stress (Pa)

Figure 7: Evolution of maximum bottom shear stress (τ_{wc}). Spatially-explicit representation of τ_{wc} in 1887 (A), 1901 (B), 1932 (C), 1970 (D), 2003 (E), 2014 (F), 2014-E25 (G), 2014-E50 (H), 2014-E75 (I), 2014-E100 (J). (K) Cumulative frequency (CDF) of τ_{wc} for the historical configurations (1887-2014). (L) Cumulative frequency of τ_{wc} in the hypothetical marsh erosion scenarios (2014-E25, E50, E75, E100)

Tidal asymmetries

Larger values of bottom shear stress increase the chance for sediments to be resuspended and transported elsewhere by tidal and wave-induced currents, thus affecting the overall lagoon sediment budget. In particular, previous studies have shown that asymmetries in tidal currents (Aubrey & Speer, 1985; Friedrichs & Aubrey, 1988) are critical in determining the ultimate fate of sediments carried in suspension, with ebb-dominated tidal flow leading to sediment export to the open sea and, therefore, to a net erosion of the lagoon (L. D'Alpaos, 2010; Finotello et al., 2019; Sarretta et al., 2010). To investigate how the lagoon's morphological changes affected tidal asymmetries (γ), we quantified the latter following the formulation proposed by Nidzieko (2010). This formulation allows for a spatially-explicit computation of γ in estuaries with mixed diurnal/semidiurnal tidal regimes based on the normalized skewness of the tidal water level time derivative ($\partial\zeta/\partial t \ = \zeta'$):

$$\gamma = \frac{\mu_3}{\sigma^3} = \frac{\frac{1}{\tau-1}\sum_{t=1}^{\tau}\left(\zeta_t' - \overline{\zeta'}\right)^3}{\left[\frac{1}{\tau-1}\sum_{t=1}^{\tau}\left(\zeta_t' - \overline{\zeta'}\right)^2\right]^{3/2}}$$

where μ_3 is the third sample moment about the mean, σ is the standard deviation, and τ is the sampling timeframe. Negative values of γ indicate ebb-dominated tides, whereas flood-dominated tides are characterized by positive values of γ. Our results suggest that progressively larger portions of the Venice Lagoon became ebb-dominated over time (Figure 8A-F). Pronounced changes in tidal asymmetry in the surroundings of the Lido inlet can be observed between 1887 and 1901 (**Figure 8**B), immediately after the construction of the jetties. Similarly, an extensive expansion of the areas dominated by ebb tides is highlighted after the construction of the jetties at the Chioggia inlet in 1932 (**Figure 8**C). Afterward, the hydrodynamic regime of many other portions of the lagoon shifted from flood- to ebb-dominated, especially around the Malamocco inlet where the Malamocco-Marghera canal was excavated (**Figure 8**D-F). Frequency distributions of γ highlight that the most pronounced changes in the hydrodynamic regime of the lagoon occurred between 1932 and 1970 (**Figure 8**K), when most of the salt marshes had already been lost and the deepening rate of tidal flats accelerated (see **Figure 2**K,L). Numerical simulations demonstrate that the effects of additional marsh losses on γ are not negligible (**Figure 8**G-J). Overall, ebb dominance is slightly reduced as salt marshes are progressively

eroded (**Figure 8**L), but distinct trends of γ changes are observed depending on the position of the individual site relative to the lagoon inlets. Specifically, while ebb-dominance is either maintained or enhanced in the portions of the lagoon closer to the inlets, a shift to flood dominance is observed in the most landward regions where extensive salt marshes are found in the present-day lagoon configuration (**Figure 8**G-J).

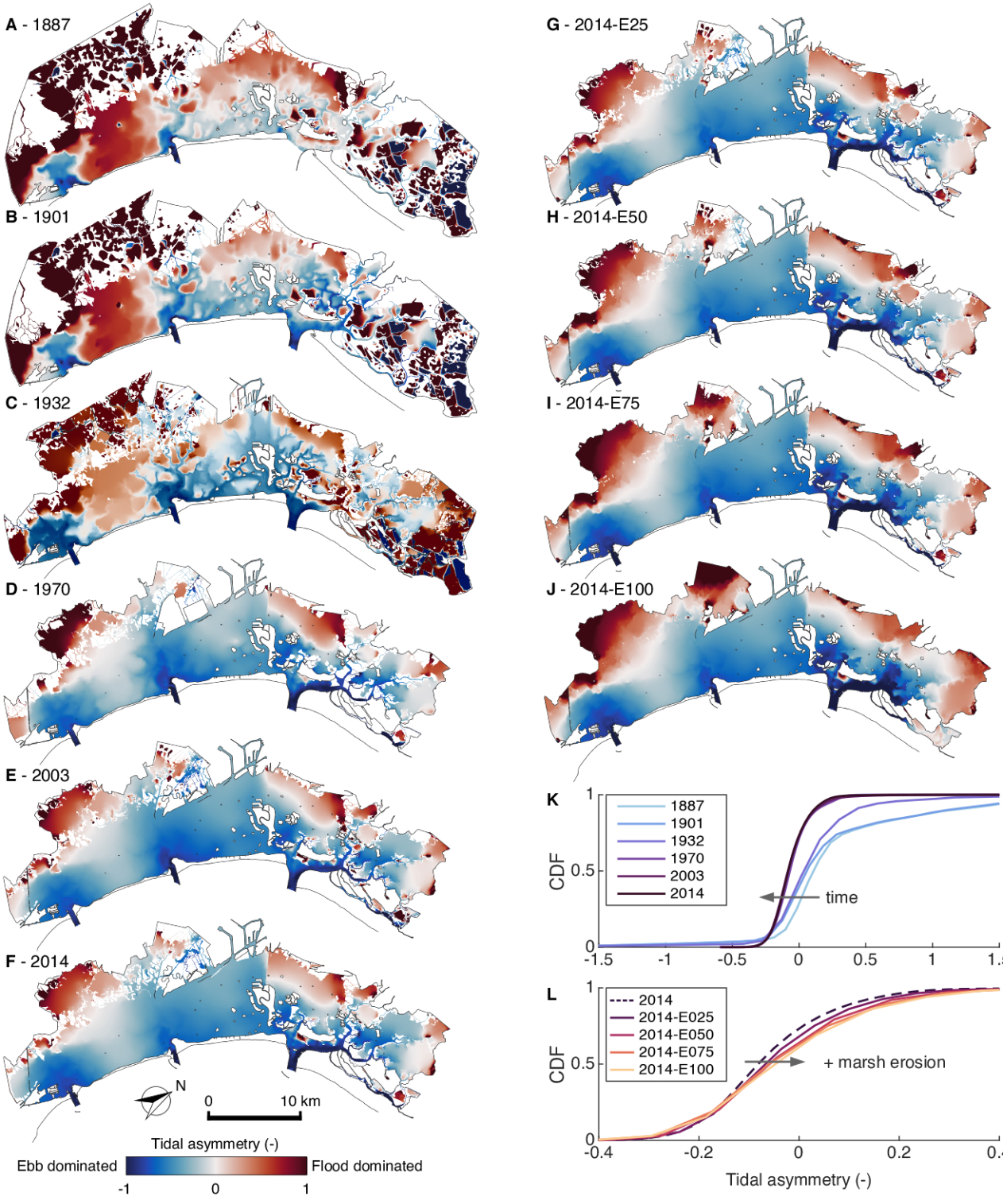
A - 1887
B - 1901
C - 1932
D - 1970
E - 2003
F - 2014
G - 2014-E25
H - 2014-E50
I - 2014-E75
J - 2014-E100
N
0
10 km
Tidal asymmetry (-)
Ebb dominated
Flood dominated
-1
0
1
K
1887
1901
1932
1970
2003
2014
CDF
time
L
2014
2014-E025
2014-E050
2014-E075
2014-E100
+ marsh erosion
Tidal asymmetry (-)

Figure 8: Evolution of tidal asymmetry (γ). Spatially-explicit representation of γ in 1887 (A), 1901 (B), 1932 (C), 1970 (D), 2003 (E), 2014 (F), 2014-E25 (G), 2014-E50 (H), 2014-E75 (I), 2014-E100 (J). (K) Cumulative frequency (CDF) of γ for the historical configurations (1887-2014). (L) Cumulative frequency of γ in the hypothetical marsh erosion scenarios (2014-E25, E50, E75, E100)

5 Discussion

Our analyses highligth the difficult task of unravelling the consequences of salt-marsh loss based exclusively on numerical results obtained for the historical configurations of the Venice Lagoon, because one can hardly isolate the direct effects of marsh disappearance on the lagoon hydrodynamics from the indirect, cascade effects due to morphodynamic feedbacks triggered by marsh loss that are all globally included in each updated configuration of the lagoon. Therefore, numerical results must be interpreted based also on the conceptualized scenarios that assume additional marsh losses without any further modifying the lagoon morphology. Again, however, caution must be given when interpretating numerical results, because the simulated scenarios could be representative of non-morphodynamic equilibrium conditions.

1. (a)

Water Levels

How marsh disappearance affects water levels within the lagoon by modifying tide propagation is perhaps the most controversial point to debate. This is because salt marshes are most effective in regulating tide propagation at high water stages (i.e., in the upper intertidal frame) due to their characteristic topographic elevations. Conversely, at lower stages, marshes are not typically flooded and thus have limited effects on tide propagation, which indeed takes place predominantly within major tidal channels and across tidal flats.

Our simulations of hypothetical marsh-loss scenarios (E25 to E100 runs, **Figure 4**L) suggest that marsh loss overall increases accommodation in the back-barrier system, thus reducing the average amplitude of tidal oscillations and, therefore, the mean tidal range ($\overline{\Delta h}$). This observation agrees with the results of the numerical experiments carried out in other back-barrier tidal systems along the continental US coast (e.g., Donatelli et al. 2018), which demonstrated, using an approach similar to that we adopted here, that tidal amplitudes are reduced when salt marshes disappear. However, our analyses also highlight a continued increase in $\overline{\Delta h}$ (Figure 4K) observed during the last century. This is most likely a result of both the anthropogenic modifications imposed on the lagoon inlets and the reduced bottom friction due to tidal flat deepening (e.g., D'Alpaos and Martini 2005; Tambroni and Seminara 2006; Carniello et al. 2009; Ferrarin et al. 2015) (Figure 2A-F). Therefore, increasing $\overline{\Delta h}$ is only partially related, both directly and indirectly, to the observed salt-marsh loss. This is supported by enhancements of $\overline{\Delta h}$ occurred in both the northern and southern lagoon immediately after the construction of jetties at the Lido (1901, Figure

4B) and Chioggia inlet (1932, Figure 4C), respectively, together with generalized increases in $\overline{\Delta h}$ between 1932 and 1970 (Figure 4D) when pronounced deepening of tidal flats took place. Excavation of the Vittorio Emanuele and Malamocco-Marghera waterways also likely contributed to promoting the observed increase in $\overline{\Delta h}$, especially in the central part of the lagoon delimited by the Malamocco inlet to the South, the city of Venice to the North, and the industrial area of Porto Marghera to the West (Figure 4C,D). Finally, slight reductions in $\overline{\Delta h}$ between 2003 and 2014 are to be related to increased hydraulic resistance at the inlets produced by the modifications associated with the Mo.S.E. works (Figure 4K) (Matticchio et al., 2017), and are therefore not directly linked to changes in salt-marsh extent.

Similarly to $\overline{\Delta h}$, the continued increase in mean high water levels (MHWL) observed since 1887 should be only partially considered as a direct effect of shrinking marsh coverage (**Figure 5**A-F). In this case, however, exploratory simulations suggest that progressive, additional loss of salt marshes would result in further MHWL increases (**Figure 5**G-J). This effect is most probably related to the progressive fading of energy dissipations produced by the presence of marshes at high-water stages. Reduced energy dissipations for high-water levels magnify tidal peaks, thus enhancing MHWL. Larger MHWL potentially bears negative consequences in terms of increased flooding risk of urban settlements (Fletcher & Spencer, 2005; Gambolati & Teatini, 2014; Rinaldo et al., 2008). One should however appreciate that marsh loss leads to differential MHWL increases across the lagoon (**Figure 5**G-J), the latter being more pronounced in the innermost portions of both the northern and central-southern lagoon where marshes are still widespread nowadays. Conversely, limited changes in MHWL are observed in the proximity of the inlets as well as around the major urban settlements found within the lagoon, namely Venice city, Chioggia, and the islands of Murano, Burano, and Sant'Erasmo. For these locations, a detailed analysis of the hypothetical scenarios of additional marsh loss highlights that changes in MHWL are lower than 3% even if marshes would entirely disappear (E100 scenario), whereas even lower variations (<2%) are found when considering the maximum, rather than the mean, high-water level (ζ_{MAX}) observed during the investigated period. Hence, the effects of salt-marsh loss on the hydrodynamics of the tidal systems which host them appears to be strongly site-specific, with significant hydrodynamic changes being observed over distances of a few kilometers even within a given tidal embayment.

Wind waves and bottom shear stresses

Differently from tidal levels, a much more straightforward interpretation can be given regarding the direct effects of marsh erosion on wind-wave fields (i.e., significant wave height $H_{s_{\mathrm{MAX}}}$, **Figure 6**) and on the associated bottom shear stresses (τ_{wc}, **Figure 7**) within the lagoon. Before 1932 the generation and propagation of large wind waves were hampered by the still-extensive presence of salt marshes (Figure 2A-C) that limited wind fetches, as well as by the reduced depths of tidal flats which promoted important wave-energy dissipation

(Figure 6A-C). From 1970 onwards, in contrast, reduced salt-marsh coverage, coupled with pronounced tidal-flat deepening, led to the observed increase in $H_{s_{\mathrm{MAX}}}$, especially in the central and southern portions of the lagoon (Figure 6D-F) (Fagherazzi et al. 2006; Defina et al. 2007). Therefore, progressively reduced marsh extent - caused also by tidal flat deepening and expansion - favors larger $H_{s_{\mathrm{MAX}}}$ due to longer fetches, as confirmed also by numerical simulations involving additional marsh loss (**Figure 6**G-J). The latter also suggests that the most significant increases in wave heights are to be expected in areas that are nowadays occupied by extensive salt marshes (i.e., the northern lagoon as well as the innermost portions of the central-southern lagoon, see Figure 2F), where the possible disappearance of salt marshes could reduce their wind-sheltering effect and increase the fetch length, eventually leading to the generation and propagation of larger waves (Figure 6G-J).

Larger $H_{S_{\mathrm{MAX}}}$ also have negative implications from a flood-risk standpoint, as higher waves could locally increase the risk of flooding due to overtopping, especially in the more topographically depressed urban areas (Gambolati & Teatini, 2014; Mel, Carniello, et al., 2021; Mel, Viero, et al., 2021; Ruol et al., 2020). Moreover, larger waves threaten the conservation of the remaining salt-marsh ecosystems, due to the positive feedback mechanism between marsh lateral erosion and wind-wave power (Carniello et al., 2016; A. D'Alpaos et al., 2013; Finotello et al., 2020; Leonardi, Defne, et al., 2016; Marani et al., 2011; Tommasini et al., 2019). Specifically, the salt-marsh lateral retreat rate is linearly correlated to wave power (P_w) (Finotello et al., 2020; Leonardi, Ganju, et al., 2016; Marani et al., 2011; Tommasini et al., 2019), which in turn is a quadratic function of wave height. Hence, salt-marsh loss leads to higher, more energetic waves which in turn enhance marsh lateral retreat even further in a superlinear fashion.

Additionally, higher waves also produce larger bottom shear stresses, especially across the extensive tidal-flat areas that characterize the lagoon morphology (**Figure 7**). Indeed, our simulations demonstrate that additional losses of salt marshes would further enhance τ_{wc} proportionally to the marsh area being lost (Figure 7G-J, L) because the wind sheltering effect typically offered by marshes would progressively be reduced, allowing for increasingly higher waves to winnow the lagoon bottom (Carniello et al., 2014, 2016; A. D'Alpaos et al., 2013; Tommasini et al., 2019). From a morphodynamic standpoint, the implications of increasing τ_{wc} can be manifold. Unquestionably, larger τ_{wc} will enhance the entrainment of fine sediment from the lagoon shallows, in this way leading to higher concentrations of suspended sediment (SSC) (Tognin et al., 2022). Notably, wave-driven resuspension from tidal flats represents a key source of sediment for salt marshes in sediment-starving shallow tidal embayments, where the majority of mineral sediments are delivered to the marsh surface during storm surge events concomitant with strong wave activity (Tognin et al., 2021). Thus, enhanced SSC could ensure higher resilience of salt-marsh ecosystems in the face of rising relative sea levels (Elsey-Quirk et al., 2019; Mariotti & Fagherazzi, 2010; Tognin et al., 2021). However, such a beneficial effect is likely to be offset

by the above-recalled marsh loss via lateral retreat, which would reduce the total marsh area and promote fragmentation, in this way hampering the marsh's ability to capture suspended sediment and cope with sea-level rise (Donatelli, Zhang, et al., 2020; Duran Vinent et al., 2021). Besides, enhanced SSC, coupled with the generally ebb-dominated character of tides (**Figure 8** and see Section 5.3), are likely to negatively affect the lagoon net-sediment budget, leading to further tidal flat deepening and salt marsh losses.

Tidal asymmetries

Loss of salt-marsh areas appears to feedback into tidal asymmetry (γ) mostly in an indirect fashion, with manmade modifications on the lagoon inlet morphologies playing, in contrast, a critical role in driving tidal asymmetry changes (L. D'Alpaos, 2010; L. D'Alpaos & Martini, 2005; Matticchio et al., 2017; Tambroni & Seminara, 2006). Indeed, pronounced γ changes are observed after the completion of the jetties at the Lido (Figure 8B) and Chioggia inlets (Figure 8C), both of which resulted in more marked ebb dominance in the inlet surroundings. Indirect effects of salt-marsh loss on γ could instead arise from the positive morphodynamic feedback between marsh loss and tidal-flat deepening (Carniello et al., 2007, 2009; Defina et al., 2007), which is likely responsible for the shift from flood- to ebb-dominance observed in many portions of the lagoon between 1932 and 1970, especially in the area facing the Malamocco inlet where the Malamocco-Marghera shipway was also excavated (Ferrarin et al., 2015) (Figure 8D-E). Nonetheless, numerical simulations demonstrate that the direct effects of additional marsh losses on tidal asymmetry are potentially not negligible, with progressive marsh erosion leading to more widespread flood-dominated areas in the innermost portions of the lagoon (Figure 8G-J). This result is consistent with evidence from previous studies showing that the decrease in intertidal storage capacity associated with gradual marsh losses will re-establish flood dominance typically observed for progressive tidal waves (Dronkers, 1986; Rinaldo et al., 1999). While enhanced flood dominance associated with marsh disappearance could potentially limit sediment export to the open sea and promote marsh accretion, one should appreciate that the tidal regime in most of the lagoon is likely to remain dominated by ebb tides, especially in the surroundings of the inlets where ebb-dominance would be even further exacerbated compared to present-day conditions (Figure 8G-J). This could hardly lead to an inversion of the ongoing net sediment loss driven by ebb-dominated tides, as sediment entrained by higher, more energetic waves will likely keep on being carried in suspension by ebb-dominated tidal currents and transported outside the lagoon for the most part. Given the non-linear dependence of sediment transport processes on both tidal flow velocities and asymmetry, however, these hypotheses should be verified by *ad hoc* coupled hydrodynamic and sediment-transport numerical simulations to investigate how sediments will be redistributed within the basin following changes in the dominant tidal regime.

Implications for the hydrodynamics of back-barrier tidal lagoons

Our analyses highlight both direct and indirect effects of salt-marsh deterioration on the hydrodynamics of the Venice Lagoon. Despite being generally consistent with previous studies carried out in different tidal settings (e.g., Donatelli et al. 2018, 2020b, a), care should be given to generalizing the results reported here to back-barrier tidal embayments morphologically and hydrodynamically different from the study case at hand. This is a general remark which holds for previous studies and should be taken into consideration for future ones.The reasons behind this caution are manyfold, though all broadly related to the morphological and hydrodynamic peculiarities that characterize each tidal environment, as well as to the conceptualization we adopted in our numerical simulations.

First, the hydrodynamic response of a tidal system to marsh erosion depends on i) the planform geometry and hypsometry of the basin (Deb et al., 2021; Van Maanen et al., 2013); ii) the characteristics of the tidal waves, especially in terms of tidal range and progressive vs. standing character of the system (Van Maanen et al., 2013; Ward et al., 2018; Zhou et al., 2018); and iii) the wave climate, affecting both the basin hydrodynamics and its sediment transport regime (Carniello et al., 2011; A. D'Alpaos et al., 2013). Particularly important is the spatial distribution of salt marshes within the back-barrier basin. As demonstrated by Donatelli et al. (2020b), different hydrodynamic changes due to marsh loss are to be expected in back-barrier systems where most marshes fringe the mainland compared to systems characterized by the presence of extensive marsh areas detached from the mainland.

Second, in our exploratory numerical simulations, we did not account for hydrodynamic changes due to rising sea levels, and assumed that marshes are ineluctably destined to disappear. In other words, we implicitly assumed that sea-level rise will outpace vertical marsh accretion, or that, more realistically, wave-driven lateral erosion will lead to marsh disappearance. This is strictly true only if the combined rate of eustatic sea-level rise and soil subsidence is higher than the rate of marsh vertical accretion, and if no significant mineral sediment supply is available from either longshore currents or fluvial sources, which could potentially allow marshes to prevent drowning and expand laterally even in the face of rising relative sea level (Ladd et al., 2019; Roner et al., 2021). Besides, salt marshes might be less vulnerable than we hypothesized even in the absence of a significant inorganic sediment supply (Kirwan et al., 2016). Indeed, even in systems characterized by negative sediment budgets, there might potentially be a transitory regime in which sediments are supplied to marshes from the adjoining, eroding tidal flats, in this way mitigating marsh drowning (Donatelli, Kalra, et al., 2020; Kalra et al., 2021; Tognin et al., 2021).

Third, our simulated scenarios do not account for the fact that salt marshes can potentially survive sea-level rise by migrating landward (e.g., Feagin et al. 2010; Field et al. 2016; Enwright et al. 2016; Fagherazzi et al. 2019; Kirwan

and Gedan 2019). While this process is hindered in the Venice Lagoon, as well as in most salt marsh ecosystems worldwide, by the presence of fixed seawalls, levees, and dikes at the interface between marshes and the upland, it cannot be disregarded *a priori*. Clearly, the colonization of new intertidal areas by marsh upland migration would profoundly change the hydrodynamics and sediment budget of the whole back-barrier system, since new areas would be periodically flooded by tides and additional sediment volumes would become available as marshes expand landward.

Finally, the timescale required for the system to morphodynamically adapt to changes in marsh coverage is generally difficult to quantify. This is because sediment volumes liberated by marsh lateral erosion can be redistributed within the basin by tidal currents and wind waves, thus affecting both the lagoon sediment budget and related morphological changes, besides potentially contributing to marsh vertical accretion (Donatelli, Kalra, et al., 2020; Elsey-Quirk et al., 2019; Kalra et al., 2021). In our simulations, in contrast, sediments eroded from marshes are instantaneously removed, and can no longer contribute to the lagoon morphological evolution. Moreover, although numerical simulations considering hypothetical scenarios may be useful to isolate the sole effects of salt-marsh loss on the hydrodynamics of back-barrier systems, it should be noted that salt-marsh loss seldom occurs without inducing modifications to other back-barrier landforms. This is clearly highlighted by historical field data from the Venice Lagoon, which suggest mutual feedback between marsh erosion and tidal-flat deepening. Therefore, generalizations of results obtained from hypothetical erosive scenarios should be treated with caution, since the modeled hydrodynamic changes could be mitigated or magnified by other morphodynamic adjustments induced by marsh disappearance on the tidal back-barrier system as a whole.

In view of the above, the effects of salt-marsh loss on the hydrodynamic and morphodynamics of shallow back-barrier tidal systems are likely to be extremely site-specific, and therefore difficult to generalize. Moreover, biogeomorphological feedbacks, which are key drivers of marsh spatiotemporal evolution, are likely to vary geographically as a consequence of distinct ecological assemblages of meta-communities and different climatic forcings. This further complicates predicting the morphodynamic effects of salt-marsh loss, as well as the timescales over which they would manifest themselves (Bertness & Ewanchuk, 2002; Finotello, Alpaos, et al., 2022; Pennings & He, 2021; Wilson et al., 2022).

6 Conclusions

In this study, we focused on the microtidal Venice Lagoon (Italy) to disentangle the role played by the loss of tidal wetlands on the hydrodynamics of tidal back-barrier embayments. Numerical simulations were performed considering both past morphological configurations of the lagoon dating back up to 1887 and hypothetical scenarios involving additional marsh erosion relative to the present-day conditions. This allowed us to highlight both direct and indirect effects of salt-marsh loss on the evolution of the lagoon hydrodynamics. Direct effects

include enhanced mean-high water levels due to reduced energy dissipation at high-water stages, as well as the formation of higher and more powerful wind waves due to longer wind fetches promoted by reduced marsh extent. Moreover, historical data and numerical results suggest that marsh disappearance is likely to trigger tidal flat deepening, thus indirectly feeding back into hydrodynamics, leading to increased tidal ranges due to reduced energy dissipation of the lagoon, and modifying tidal asymmetries across the entire back-barrier system. We also speculated on the potential impacts of the observed hydrodynamic changes on the lagoon ecomorphodynamic evolution, as well as on the associated risk of tidal flooding in urban settlements. Although further investigations will be needed to conclusively address these hypotheses, our analyses suggest that in the absence of sea-level rise, further losses of salt marshes are unlikely to critically affect urban flooding risk, whereas it may promote additional marsh lateral erosion through positive feedback between reduced marsh extent and higher wind-wave power.

The findings of this study provide novel insights into the hydrodynamic effects of salt-marsh loss in sediment-starving, shallow tidal embayments morphodynamically dominated by wind-driven sediment transport processes, with far-reaching implications for the conservation and restoration of coastal ecosystems that extend well beyond the study case at hand. However, we stress that care should be given to generalizing the results presented here to tidal embayments that are morphologically and morphodynamically different from the Venice Lagoon. In doing so, we support the idea that the response of back-barrier systems to changing external forcing is highly dependent on site-specific morphological and ecological features, as well as on the characteristic of the local tide, wave, climate, and fluvial processes. This clearly prevents one from drawing general conclusions regarding the future of coastal back-barrier systems worldwide based on the analyses of individual study cases.

Acknowledgments

[reviewers will be acknowledged]. This scientific activity was performed in the Research Programme Venezia2021, with the contribution of the Provveditorato for the Public Works of Veneto, Trentino Alto Adige and Friuli Venezia Giulia, provided through the concessionary of State Consorzio Venezia Nuova and coordinated by CORILA, Research Line 3.2 (PI Andrea D'Alpaos).

Author contributions

Conceptualization: Alvise Finotello, Davide Tognin, Andrea D'Alpaos, Luca Carniello;
Methodology: Alvise Finotello, Davide Tognin, Andrea D'Alpaos, Luca Carniello;
Formal analysis and investigation: Alvise Finotello, Davide Tognin;
Figures: Davide Tognin;
Writing - original draft preparation: Alvise Finotello, Davide Tognin;
Writing - review and editing: all authors;

Funding acquisition: Andrea D'Alpaos, Luca Carniello, Enrico Bertuzzo;
Resources: Andrea D'Alpaos, Luca Carniello, Enrico Bertuzzo, Massimiliano Ghinassi;
Supervision: Andrea D'Alpaos, Luca Carniello, Enrico Bertuzzo.

Open Research

All data needed to evaluate the results presented in the paper can be found at http://researchdata.cab.unipd.it/id/eprint/646. Meteorological data for the Venice Lagoon are also freely available at www.comune.venezia.it/content/dati-dalle-stazioni-rilevamento and www.venezia.isprambiente.it/rete-meteo-mareografica.

References

Amos, C. L., Umgiesser, G., Tosi, L., & Townend, I. H. (2010). The coastal morphodynamics of Venice lagoon, Italy: An introduction. *Continental Shelf Research*, *30*(8), 837–846. https://doi.org/10.1016/j.csr.2010.01.014Aubrey, D. G., & Speer, P. E. (1985). A study of non-linear tidal propagation in shallow inlet/estuarine systems Part I: Observations. *Estuarine, Coastal and Shelf Science*, *21*(2), 185–205. https://doi.org/https://doi.org/10.1016/0272-7714(85)90096-4Barbier, E. B., Hacker, S. D., Kennedy, C., Koch, E. W., Stier, A. C., & Silliman, B. R. (2011). The value of estuarine and coastal ecosystem services. *Ecological Monographs*, *81*(2), 169–193. https://doi.org/10.1890/10-1510.1Bertness, M. D., & Ewanchuk, P. J. (2002). Latitudinal and climate-driven variation in the strength and nature of biological interactions in New England salt marshes. *Oecologia*, *132*(3), 392–401. https://doi.org/10.1007/s00442-002-0972-yBoothroyd, J. C., Friedrich, N. E., & McGinn, S. R. (1985). Geology of microtidal coastal lagoons: Rhode Island. *Marine Geology*, *63*(1), 35–76. https://doi.org/https://doi.org/10.1016/0025-3227(85)90079-9Carbognin, L., Teatini, P., & Tosi, L. (2004). Eustacy and land subsidence in the Venice Lagoon at the beginning of the new millennium. *Journal of Marine Systems*, *51*(1-4 SPEC. ISS.), 345–353. https://doi.org/10.1016/j.jmarsys.2004.05.021Carniello, L., Defina, A., Fagherazzi, S., & D'Alpaos, L. (2005). A combined wind wave-tidal model for the Venice lagoon, Italy. *Journal of Geophysical Research: Earth Surface*, *110*(4), 1–15. https://doi.org/10.1029/2004JF000232Carniello, L., D'Alpaos, L., Defina, A., & Fagherazzi, S. (2007). A conceptual model for the long term evolution of tidal flats in the Venice lagoon. *River, Coastal and Estuarine Morphodynamics*, 137–144.Carniello, L., Defina, A., & D'Alpaos, L. (2009). Morphological evolution of the Venice lagoon: Evidence from the past and trend for the future. *Journal of Geophysical Research: Earth Surface*, *114*(4), 1–10. https://doi.org/10.1029/2008JF001157Carniello, L., D'Alpaos, A., & Defina, A. (2011). Modeling wind waves and tidal flows in shallow micro-tidal basins. *Estuarine, Coastal and Shelf Science*, *92*(2), 263–276. https://doi.org/10.1016/j.ecss.2011.01.001Carniello, L., Defina, A., D'Alpaos, L., & D'Alpaos, L. (2012). Modeling sand-mud transport induced by tidal currents and wind waves in shallow microtidal basins: Application to the

Venice Lagoon (Italy). *Estuarine, Coastal and Shelf Science*, *102–103*, 105–115. https://doi.org/10.1016/j.ecss.2012.03.016Carniello, L., Silvestri, S., Marani, M., D'Alpaos, A., Volpe, V., & Defina, A. (2014). Sediment dynamics in shallow tidal basins: In situ observations, satellite retrievals, and numerical modeling in the Venice Lagoon. *Journal of Geophysical Research: Earth Surface*, *119*(4), 802–815. https://doi.org/10.1002/2013JF003015Carniello, L., D'Alpaos, A., Botter, G., & Rinaldo, A. (2016). Statistical characterization of spatio-temporal sediment dynamics in the Venice lagoon. *Journal of Geophysical Research: Earth Surface*, *121*(January), 1049–1064. https://doi.org/10.1002/2015JF003793Carson, B., Ashley, G. M., Lennon, G. P., Weisman, R. N., Nadeau, J. E., Hall, M. J., et al. (1988). Hydrodynamics and sedimentation in a back-barrier lagoon-salt marsh system, Great Sound, New Jersey — A summary. *Marine Geology*, *82*(1), 123–132. https://doi.org/https://doi.org/10.1016/0025-3227(88)90011-4Chmura, G. L., Anisfeld, S. C., Cahoon, D. R., & Lynch, J. C. (2003). Global carbon sequestration in tidal, saline wetland soils. *Global Biogeochemical Cycles*, *17*(4), 21–22. https://doi.org/10.1029/2002gb001917Costanza, R., D'Arge, R., De Groot, R., Farber, S., Grasso, M., Hannon, B., et al. (1997). The value of the world's ecosystem services and natural capital. *Nature*, *387*(6630), 253–260. https://doi.org/10.1038/387253a0D'Alpaos, A., Lanzoni, S., Marani, M., & Rinaldo, A. (2007). Landscape evolution in tidal embayments: Modeling the interplay of erosion, sedimentation, and vegetation dynamics. *Journal of Geophysical Research: Earth Surface*, *112*(1), 1–17. https://doi.org/10.1029/2006JF000537D'Alpaos, A., Carniello, L., & Rinaldo, A. (2013). Statistical mechanics of wind wave-induced erosion in shallow tidal basins: Inferences from the Venice Lagoon. *Geophysical Research Letters*, *40*(13), 3402–3407. https://doi.org/10.1002/grl.50666D'Alpaos, C., & D'Alpaos, A. (2021). The Valuation of Ecosystem Services in the Venice Lagoon: A Multicriteria Approach. *Sustainability*, *13*(17), 9485. https://doi.org/10.3390/su13179485D'Alpaos, L. (2010). *Fatti e misfatti di idraulica lagunare. La laguna di Venezia dalla diversione dei fiumi alle nuove opere delle bocche di porto. Istituto Veneto di Scienze, Lettere e Arti*. Venice: Istituto Veneto di Scienze, Lettere ed Arti.D'Alpaos, L., & Defina, A. (2007). Mathematical modeling of tidal hydrodynamics in shallow lagoons: A review of open issues and applications to the Venice lagoon. *Computers and Geosciences*, *33*(4), 476–496. https://doi.org/10.1016/j.cageo.2006.07.009D'Alpaos, L., & Martini, P. (2005). The influence of the inlet configuration on sediment loss in the Venice Lagoon. In C. A. Fletcher & T. Spencer (Eds.), *Flooding and Environmental Challanges for Venice and its Lagoon: State of Knowledge* (p. 691). Cambridge: Cambridge University Press.Deb, M., Abdolali, A., Kirby, J. T., Shi, F., Guiteras, S., & McDowell, C. (2021). Sensitivity of tidal hydrodynamics to varying bathymetric configurations in a multi-inlet rapidly eroding salt marsh system: A numerical study. *Earth Surface Processes and Landforms*, (November 2021), 1157–1182. https://doi.org/10.1002/esp.5308Defina, A. (2000). Two-dimensional shallow flow equations for partially dry areas. *Water Resources Research*, *36*(11),

3251. https://doi.org/10.1029/2000WR900167Defina, A. (2003). Numerical experiments on bar growth. *Water Resources Research*, *39*(4), 1–12. https://doi.org/10.1029/2002WR001455Defina, A., Carniello, L., Fagherazzi, S., & D'Alpaos, L. (2007). Self-organization of shallow basins in tidal flats and salt marshes. *Journal of Geophysical Research: Earth Surface*, *112*(3), 1–11. https://doi.org/10.1029/2006JF000550Donatelli, C. (2020). *Large-Scale Effects Induced By Salt Marsh And Seagrass Loss In Shallow Tidal Lagoons. Orphanet Journal of Rare Diseases*. Ph.D Dissertation. University of Liverpool. https://doi.org/10.17638/03093180Donatelli, C., Ganju, N. K., Zhang, X., Fagherazzi, S., & Leonardi, N. (2018). Salt Marsh Loss Affects Tides and the Sediment Budget in Shallow Bays. *Journal of Geophysical Research: Earth Surface*, *123*(10), 2647–2662. https://doi.org/10.1029/2018JF004617Donatelli, C., Zhang, X., Ganju, N. K., Aretxabaleta, A. L., Fagherazzi, S., & Leonardi, N. (2020). A nonlinear relationship between marsh size and sediment trapping capacity compromises salt marshes' stability. *Geology*, *48*(10), 966–970. https://doi.org/10.1130/G47131.1Donatelli, C., Kalra, T. S., Fagherazzi, S., Zhang, X., & Leonardi, N. (2020). Dynamics of Marsh-Derived Sediments in Lagoon-Type Estuaries. *Journal of Geophysical Research: Earth Surface*, *125*(12). https://doi.org/10.1029/2020JF005751Dronkers, J. (1986). Tidal asymmetry and estuarine morphology. *Netherlands Journal of Sea Research*, *20*(2–3), 117–131. https://doi.org/10.1016/0077-7579(86)90036-0Duran Vinent, O., Herbert, E. R., Coleman, D. J., Himmelstein, J. D., & Kirwan, M. L. (2021). Onset of runaway fragmentation of salt marshes. *One Earth*, *4*(4), 506–516. https://doi.org/10.1016/j.oneear.2021.02.013Elsey-Quirk, T., Mariotti, G., Valentine, K., & Raper, K. (2019). Retreating marsh shoreline creates hotspots of high-marsh plant diversity. *Scientific Reports*, *9*(1), 1–9. https://doi.org/10.1038/s41598-019-42119-8Enwright, N. M., Griffith, K. T., & Osland, M. J. (2016). Barriers to and opportunities for landward migration of coastal wetlands with sea-level rise. *Frontiers in Ecology and the Environment*, *14*(6), 307–316. https://doi.org/https://doi.org/10.1002/fee.1282Fagherazzi, S., Kirwan, M. L., Mudd, S. M., Guntenspergen, G. R., Temmerman, S., D'Alpaos, A., et al. (2012). Numerical models of salt marsh evolution: Ecological, geomorphic, and climatic factors. *Reviews of Geophysics*, *50*(1), 1–28. https://doi.org/10.1029/2011RG000359Fagherazzi, S., Anisfeld, S. C., Blum, L. K., Long, E. V., Feagin, R. A., Fernandes, A., et al. (2019). Sea level rise and the dynamics of the marsh-upland boundary. *Frontiers in Environmental Science*, *7*(FEB), 1–18. https://doi.org/10.3389/fenvs.2019.00025Feagin, R. A., Martinez, M. L., Mendoza-Gonzalez, G., & Costanza, R. (2010). Salt marsh zonal migration and ecosystem service change in response to global sea level rise: A case study from an urban region. *Ecology and Society*, *15*(4). https://doi.org/10.5751/ES-03724-150414Ferrarin, C., Tomasin, A., Bajo, M., Petrizzo, A., & Umgiesser, G. (2015). Tidal changes in a heavily modified coastal wetland. *Continental Shelf Research*, *101*, 22–33. https://doi.org/10.1016/j.csr.2015.04.002Field, C. R., Gjerdrum, C., & Elphick, C. S. (2016). Forest resistance to sea-level rise prevents landward migration of tidal marsh. *Biological Conservation*, *201*, 363–369.

https://doi.org/https://doi.org/10.1016/j.biocon.2016.07.035Finkelstein, K., & Ferland, M. A. (1987). Back-barrier response to sea-level rise, eastern shore of Virginia. *Sea-Level Fluctuation and Coastal Evolution*, 145–155. https://doi.org/10.2110/pec.87.41.0145Finotello, A., Canestrelli, A., Carniello, L., Ghinassi, M., & D'Alpaos, A. (2019). Tidal flow asymmetry and discharge of lateral tributaries drive the evolution of a microtidal meander in the Venice Lagoon (Italy). *Journal of Geophysical Research: Earth Surface*, *124*(12), 3043–3066. https://doi.org/10.1029/2019jf005193Finotello, A., Marani, M., Carniello, L., Pivato, M., Roner, M., Tommasini, L., & D'Alpaos, A. (2020). Control of wind-wave power on morphological shape of salt marsh margins. *Water Science and Engineering*, *13*(1), 45–56. https://doi.org/10.1016/j.wse.2020.03.006Finotello, A., Alpaos, A. D., Marani, M., & Bertuzzo, E. (2022). A Minimalist Model of Salt-Marsh Vegetation Dynamics Driven by Species Competition and Dispersal. *Frontiers in Marine*, *9*(866570), 1–23. https://doi.org/10.3389/fmars.2022.866570Finotello, A., Capperucci, R. M., Bartholomä, A., D'Alpaos, A., & Ghinassi, M. (2022). Morpho-sedimentary evolution of a microtidal meandering channel driven by 130-years of natural and anthropogenic modifications of the Venice Lagoon (Italy). *Earth Surface Processes and Landforms*, *n/a*(n/a). https://doi.org/https://doi.org/10.1002/esp.5396FitzGerald, D. M., & Hughes, Z. (2019). Marsh Processes and Their Response to Climate Change and Sea-Level Rise. *Annual Review of Earth and Planetary Sciences*, *47*(1), 481–517. https://doi.org/10.1146/annurev-earth-082517-010255Flemming, B. W. (2012). *Geology, Morphology, and Sedimentology of Estuaries and Coasts*. *Treatise on Estuarine and Coastal Science* (Vol. 3). Elsevier Inc. https://doi.org/10.1016/B978-0-12-374711-2.00302-8Fletcher, C. A., & Spencer, T. (2005). *Flooding and environmental challenges for Venice and its lagoon: State of knowledge*. (C. A. Fletcher & T. Spencer, Eds.) (Cambridge). Cambridge, UK.Friedrichs, C. T., & Aubrey, D. G. (1988). Nonlinear tidal distortion in shallow well-mixed estuaries: a synthesis. *Estuarine, Coastal and Shelf Science*, *27*(3), 521–545. https://doi.org/10.1016/0272-7714(90)90054-UGambolati, G., & Teatini, P. (2014). *Venice Shall Rise Again -Engineered Uplift of Venice Through Seawater Injection*. *Elsevier Insights [electronic]*. Amsterdam, Netherlands: Elsevier. https://doi.org/10.1016/B978-0-12-420144-6.00005-4Gatto, P., & Carbognin, L. (1981). The lagoon of Venice: Natural environmental trend and man-induced modification. *Hydrological Sciences Bulletin*, *26*(4), 379–391. https://doi.org/10.1080/02626668109490902Ghezzo, M., Guerzoni, S., Cucco, A., & Umgiesser, G. (2010). Changes in Venice Lagoon dynamics due to construction of mobile barriers. *Coastal Engineering*, *57*(7), 694–708. https://doi.org/10.1016/j.coastaleng.2010.02.009Gilby, B. L., Weinstein, M. P., Baker, R., Cebrian, J., Alford, S. B., Chelsky, A., et al. (2021). Human Actions Alter Tidal Marsh Seascapes and the Provision of Ecosystem Services. *Estuaries and Coasts*, *44*(6), 1628–1636. https://doi.org/10.1007/s12237-020-00830-0González-Villanueva, R., Pérez-Arlucea, M., Costas, S., Bao, R., Otero, X. L., & Goble, R. (2015). 8000 years of environmental evolution of barrier–lagoon systems emplaced

in coastal embayments (NW Iberia). *The Holocene*, *25*(11), 1786–1801. https://doi.org/10.1177/0959683615591351Gourgue, O., van Belzen, J., Schwarz, C., Vandenbruwaene, W., Vanlede, J., Belliard, J.-P., et al. (2021). Biogeomorphic modeling to assess resilience of tidal marsh restoration to sea level rise and sediment supply. *Earth Surface Dynamics Discussions*, (October), 1–38. https://doi.org/10.5194/esurf-2021-66Green, M. O., & Coco, G. (2014). Review of wave-driven sediment resuspension and transport in estuaries. *Reviews of Geophysics*. https://doi.org/10.1002/2013RG000437Hesp, P. A. (2016). Coastal Barriers. In M. J. Kennish (Ed.), *Encyclopedia of Estuaries* (pp. 128–130). Dordrecht: Springer Netherlands. https://doi.org/10.1007/978-94-017-8801-4_279Holthuijsen, L. H., Booij, N., & Herbers, T. H. C. (1989). A prediction model for stationary, short-crested waves in shallow water with ambient currents. *Coastal Engineering*, *13*(1), 23–54. https://doi.org/10.1016/0378-3839(89)90031-8Hughes, Z. J., FitzGerald, D. M., & Wilson, C. A. (2021). Impacts of Climate Change and Sea Level Rise. In D. M. FitzGerald & Z. J. Hughes (Eds.), *Salt Marshes: Function, Dynamics, and Stresses* (pp. 476–481). Cambridge: Cambridge University Press. https://doi.org/DOI: 10.1017/9781316888933.021Kalra, T. S., Ganju, N. K., Aretxabaleta, A. L., Carr, J. A., Defne, Z., & Moriarty, J. M. (2021). Modeling Marsh Dynamics Using a 3-D Coupled Wave-Flow-Sediment Model. *Frontiers in Marine Science*, *8*(November). https://doi.org/10.3389/fmars.2021.740921Kennish, M. J. (2016). Coastal Lagoons. In M. J. Kennish (Ed.), *Encyclopedia of Estuaries* (pp. 140–143). Dordrecht: Springer Netherlands. https://doi.org/10.1007/978-94-017-8801-4_47Kirwan, M. L., & Gedan, K. B. (2019). Sea-level driven land conversion and the formation of ghost forests. *Nature Climate Change*, *9*(6), 450–457. https://doi.org/10.1038/s41558-019-0488-7Kirwan, M. L., Temmerman, S., Skeehan, E. E., Guntenspergen, G. R., & Fagherazzi, S. (2016). Overestimation of marsh vulnerability to sea level rise. *Nature Climate Change*, *6*(3), 253–260. https://doi.org/10.1038/nclimate2909Ladd, C. J. T., Duggan-Edwards, M. F., Bouma, T. J., Pagès, J. F., & Skov, M. W. (2019). Sediment Supply Explains Long-Term and Large-Scale Patterns in Salt Marsh Lateral Expansion and Erosion. *Geophysical Research Letters*, *46*(20), 11178–11187. https://doi.org/10.1029/2019GL083315Leonardi, N., Ganju, N. K., & Fagherazzi, S. (2016). A linear relationship between wave power and erosion determines salt-marsh resilience to violent storms and hurricanes. *Proceedings of the National Academy of Sciences*, *113*(1), 64–68. https://doi.org/10.1073/pnas.1510095112Leonardi, N., Defne, Z., Ganju, N. K., & Fagherazzi, S. (2016). Salt marsh erosion rates and boundary features in a shallow Bay. *Journal of Geophysical Research : Earth Surface*, *121*(10), 1–15. https://doi.org/10.1002/2016JF003975.ReceivedLevin, L. A., Boesch, D. F., Covich, A., Dahm, C., Erséus, C., Ewel, K. C., et al. (2001). The function of marine critical transition zones and the importance of sediment biodiversity. *Ecosystems*, *4*(5), 430–451. https://doi.org/10.1007/s10021-001-0021-4Van Maanen, B., Coco, G., & Bryan, K. R. (2013). Modelling the effects of tidal range and initial bathymetry on the morphological evolution of tidal embayments. *Geomorphology*, *191*,

23–34. https://doi.org/10.1016/j.geomorph.2013.02.023Marani, M., D'Alpaos, A., Lanzoni, S., & Santalucia, M. (2011). Understanding and predicting wave erosion of marsh edges. *Geophysical Research Letters*, *38*(21), 1–5. https://doi.org/10.1029/2011GL048995Mariotti, G. (2020). Beyond marsh drowning: The many faces of marsh loss (and gain). *Advances in Water Resources*, *144*(July), 103710. https://doi.org/10.1016/j.advwatres.2020.103710Mariotti, G., & Carr, J. A. (2014). Dual role of salt marsh retreat: Long-term loss and short-term resilience. *Water Resources Research*, *50*(4), 2963–2974. https://doi.org/10.1002/2013WR014333.ReceivedMariotti, G., & Fagherazzi, S. (2010). A numerical model for the coupled long-term evolution of salt marshes and tidal flats. *Journal of Geophysical Research: Earth Surface*, *115*(F1). https://doi.org/https://doi.org/10.1029/2009JF001326Mariotti, G., & Fagherazzi, S. (2013). Critical width of tidal flats triggers marsh collapse in the absence of sea-level rise. *Proceedings of the National Academy of Sciences of the United States of America*, *110*(14), 5353–6. https://doi.org/10.1073/pnas.1219600110Matticchio, B., Carniello, L., Canesso, D., Ziggiotto, E., & Cordella, M. (2017). Recent changes in tidal propagation in the Venice Lagoon: effects of changes in the inlet structure. In L. D'Alpaos (Ed.), *Commissione di studio sui problemi di Venezia, Volume III: La laguna di Venezia e le nuove opere alle bocche* (Istituto V, pp. 157–183). Venice: Istituto Veneto di Scienze, Lettere ed Arti.Mcowen, C. J., Weatherdon, L. V., Van Bochove, J.-W. J. W., Sullivan, E., Blyth, S., Zockler, C., et al. (2017). A global map of saltmarshes. *Biodiversity Data Journal*, *5*(1). https://doi.org/10.3897/BDJ.5.e11764Mel, R. A., Carniello, L., & D'alpaos, L. (2021). How long the Mo.S.E. barriers will be effective in protecting all the urban settlements in the Venice lagoon? The wind setup constraint. *Coastal Engineering*, *168*(January), 103923. https://doi.org/10.1016/j.coastaleng.2021.103923Mel, R. A., Viero, D. P., Carniello, L., Defina, A., & D'Alpaos, L. (2021). The first operations of Mo.S.E. system to prevent the flooding of Venice: Insights on the hydrodynamics of a regulated lagoon. *Estuarine, Coastal and Shelf Science*, *261*(August), 107547. https://doi.org/10.1016/j.ecss.2021.107547Mitsch, W. J., & Gosselink, J. G. (2000). The value of wetlands: importance of scale and landscape setting. *Ecological Economics*, *35*(1), 25–33. https://doi.org/10.1016/S0921-8009(00)00165-8Mitsch, W. J., Bernal, B., & Hernandez, M. E. (2015). Ecosystem services of wetlands. *International Journal of Biodiversity Science, Ecosystem Services and Management*, *11*(1), 1–4. https://doi.org/10.1080/21513732.2015.1006250Möller, I., Kudella, M., Rupprecht, F., Spencer, T., Paul, M., Van Wesenbeeck, B. K. B. K., et al. (2014). Wave attenuation over coastal salt marshes under storm surge conditions. *Nature Geoscience*, *7*(10), 727–731. https://doi.org/10.1038/NGEO2251Nelson, J. L., & Zavaleta, E. S. (2012). Salt marsh as a coastal filter for the oceans: Changes in function with experimental increases in Nitrogen loading and sea-level rise. *PLoS ONE*, *7*(8). https://doi.org/10.1371/journal.pone.0038558Nidzieko, N. J. (2010). Tidal asymmetry in estuaries with mixed semidiurnal/diurnal tides. *Journal of Geo-*

physical Research: Oceans, *115*(8), 1–13. https://doi.org/10.1029/2009JC005864Passeri, D. L., Dalyander, P. S., Long, J. W., Mickey, R. C., Jenkins III, R. L., Thompson, D. M., et al. (2020). The Roles of Storminess and Sea Level Rise in Decadal Barrier Island Evolution. *Geophysical Research Letters*, *47*(18), e2020GL089370. https://doi.org/https://doi.org/10.1029/2020GL089370Pennings, S. C., & He, Q. (2021). Community Ecology of Salt Marshes. In D. M. FitzGerald & Z. J. Hughes (Eds.), *Salt Marshes: Function, Dynamics, and Stresses* (pp. 82–112). Cambridge: Cambridge University Press. https://doi.org/DOI: 10.1017/9781316888933.006Pérez-Ruzafa, A., Pérez-Ruzafa, I. M., Newton, A., & Marcos, C. (2019). Coastal Lagoons: Environmental Variability, Ecosystem Complexity, and Goods and Services Uniformity. In E. Wolanski, J. W. Day, M. Elliott, & R. Ramachandran (Eds.), *Coasts and Estuaries* (pp. 253–276). Amsterdam, Netherlands: Elsevier. https://doi.org/https://doi.org/10.1016/B978-0-12-814003-1.00015-0Perillo, G. M. E. (1995). Geomorphology and Sedimentology of Estuaries: An Introduction. In G. M. E. Perillo (Ed.), *Geomorphology and Sedimentology of Estuaries* (Vol. 53, pp. 1–16). Amsterdam, Netherlands: Elsevier. https://doi.org/https://doi.org/10.1016/S0070-4571(05)80021-4Perillo, G. M. E., Wolanski, E., Brinson, M. M., Cahoon, D. R., & Hopkinson, C. S. (2019). *Coastal wetlands : A Synthesis*. (G. Perillo, E. Wolanski, D. R. Cahoon, & C. S. Hopkinson, Eds.), *Coastal wetlands : an integrated ecosystem approach*. Amsterdam, Netherlands: Elsevier.Peter Sheng, Y., Paramygin, V. A., Rivera-Nieves, A. A., Zou, R., Fernald, S., Hall, T., & Jacob, K. (2022). Coastal marshes provide valuable protection for coastal communities from storm-induced wave, flood, and structural loss in a changing climate. *Scientific Reports*, *12*(1), 1–12. https://doi.org/10.1038/s41598-022-06850-zPollard, J. A., Spencer, T., & Brooks, S. M. (2019). The interactive relationship between coastal erosion and flood risk. *Progress in Physical Geography*, *43*(4), 574–585. https://doi.org/10.1177/0309133318794498Rinaldo, A., Fagherazzi, S., Lanzoni, S., Marani, M., & Dietrich, W. E. (1999). Tidal networks 3. Landscape-forming discharges and studies in empirical geomorphic relationships. *Water Resources Research*, *35*(12), 3919–3929. https://doi.org/10.1029/1999WR900238Rinaldo, A., Nicotina, L., Alessi Celegon, E., Beraldin, F., Botter, G., Carniello, L., et al. (2008). Sea level rise, hydrologic runoff, and the flooding of Venice. *Water Resources Research*, *44*(12), 1–12. https://doi.org/10.1029/2008WR007195Roner, M., Ghinassi, M., Finotello, A., Bertini, A., Combourieu-nebout, N., Donnici, S., et al. (2021). Detecting the Delayed Signatures of Changing Sediment Supply in Salt-Marsh Landscapes : The Case of the Venice Lagoon (Italy). *Frontiers in Marine Science*, *8:742603*. https://doi.org/10.3389/fmars.2021.742603Ruol, P., Favaretto, C., Volpato, M., & Martinelli, L. (2020). Flooding of Piazza San Marco (Venice): Physical model tests to evaluate the overtopping discharge. *Water (Switzerland)*, *12*(2). https://doi.org/10.3390/w12020427Sarretta, A., Pillon, S., Molinaroli, E., Guerzoni, S., & Fontolan, G. (2010). Sediment budget in the Lagoon of Venice, Italy. *Continental Shelf Research*, *30*(8), 934–949. https://doi.org/10.1016/j.csr.2009.07.002Silvestri, S., D'Alpaos, A., Nordio, G., & Carniello, L. (2018). Anthropogenic Modifications Can Significantly Influence the Local Mean Sea Level and Affect the Survival of Salt Marshes in Shallow

Tidal Systems. *Journal of Geophysical Research: Earth Surface*, *123*(5), 996–1012. https://doi.org/10.1029/2017JF004503Smagorinsky, J. (1963). General circulation experiments with the primitive equations: I. the basic experiment. *Monthly Weather Review*, *91*(3), 99–164. https://doi.org/10.1175/1520-0493(1963)091<0099:GCEWTP>2.3.CO;2Soulsby, R. L. (1995). Bed shear-stresses due to combined waves and currents. In M. J. F. et al Stive (Ed.), *Advances in Coastal Morphodynamics* (pp. 4-20-4–23). Delft Hydraul., Delft, Netherlands.Stutz, M. L., & Pilkey, O. H. (2011). Open-Ocean Barrier Islands: Global Influence of Climatic, Oceanographic, and Depositional Settings. *Journal of Coastal Research*, *27*(2), 207–222. https://doi.org/10.2112/09-1190.1De Swart, H. E., & Zimmerman, J. T. F. (2009). Morphodynamics of Tidal Inlet Systems. *Annual Review of Fluid Mechanics*, *41*(1), 203–229. https://doi.org/10.1146/annurev.fluid.010908.165159Tambroni, N., & Seminara, G. (2006). Are inlets responsible for the morphological degradation of Venice Lagoon? *Journal of Geophysical Research: Earth Surface*, *111*(3), 1–19. https://doi.org/10.1029/2005JF000334Temmerman, S., Meire, P., Bouma, T. J. T. J., Herman, P. M. J. P. M. J., Ysebaert, T., De Vriend, H. J., & Vriend, H. J. De. (2013). Ecosystem-based coastal defence in the face of global change. *Nature*, *504*(7478), 79–83. https://doi.org/10.1038/nature12859Tognin, D., D'Alpaos, A., Marani, M., & Carniello, L. (2021). Marsh resilience to sea-level rise reduced by storm-surge barriers in the Venice Lagoon. *Nature Geoscience*, *14*(12), 906–911. https://doi.org/10.1038/s41561-021-00853-7Tognin, D., Finotello, A., D'Alpaos, A., Viero, D. P., Pivato, M., Mel, R. A., et al. (2022). Loss of geomorphic diversity in shallow tidal embayments promoted by storm-surge barriers. *Science Advances*, *8*(13). https://doi.org/10.1126/sciadv.abm844Tomasin, A. (1974). Recent changes in the tidal regime in Venice. *Rivista Italiana Di Geofisica*, *23*(5/6), 275–278.Tommasini, L., Carniello, L., Ghinassi, M., Roner, M., & D'Alpaos, A. (2019). Changes in the wind-wave field and related salt-marsh lateral erosion: inferences from the evolution of the Venice Lagoon in the last four centuries. *Earth Surface Processes and Landforms*, *44*(8), 1633–1646. https://doi.org/10.1002/esp.4599Valiela, I., Kinney, E., Culberston, J., Peacock, E., & Smith, S. (2009). Global Losses of Mangroves and Salt Marshes. In C. M. Duarte (Ed.), *Global Loss of Coastal Habitats: Rates, Causes and Consequences* (Fundacion, p. 184). Bilbao.Valle-Levinson, A., Marani, M., Carniello, L., D'Alpaos, A., & Lanzoni, S. (2021). Astronomic link to anomalously high mean sea level in the northern Adriatic Sea. *Estuarine, Coastal and Shelf Science*, *257*, 107418. https://doi.org/https://doi.org/10.1016/j.ecss.2021.107418Ward, S. L., Robins, P. E., Lewis, M. J., Iglesias, G., Hashemi, M. R., & Neill, S. P. (2018). Tidal stream resource characterisation in progressive versus standing wave systems. *Applied Energy*, *220*(October 2017), 274–285. https://doi.org/10.1016/j.apenergy.2018.03.059Wei, Y., Chen, Y., Qiu, J., Zhou, Z., Yao, P., Jiang, Q., et al. (2022). The role of geological mouth islands on the morphodynamics of back-barrier tidal basins. *Earth Surface Dynamics*, *10*(1), 65–80. https://doi.org/10.5194/esurf-10-65-2022Willemsen,

P. W. J. M., Smits, B. P., Borsje, B. W., Herman, P. M. J., Dijkstra, J. T., Bouma, T. J., & Hulscher, S. J. M. H. (2021). Modelling decadal salt marsh development: variability of the salt marsh edge under influence of waves and sediment availability. *Water Resources Research*, *58*, e2020WR028962. https://doi.org/https://doi.org/10.1029/2020WR028962Wilson, C. A., Hughes, Z. J., & FitzGerald, D. M. (2022). Causal relationships among sea level rise, marsh crab activity, and salt marsh geomorphology. *Proceedings of the National Academy of Sciences*, *119*(9), e2111535119. https://doi.org/10.1073/pnas.2111535119Young, I. R. R., & Verhagen, L. A. A. (1996). The growth of fetch-limited waves in water of finite depth. Part 1: Total energy and peak frequency. *Coastal Engineering*, *29*(1–2), 47–78.Zanchettin, D., Bruni, S., Raicich, F., Lionello, P., Adloff, F., Androsov, A., et al. (2021). Sea-level rise in Venice: Historic and future trends (review article). *Natural Hazards and Earth System Sciences*, *21*(8), 2643–2678. https://doi.org/10.5194/nhess-21-2643-2021Zarzuelo, C., López-Ruiz, A., D'Alpaos, A., Carniello, L., & Ortega-Sánchez, M. (2018). Assessing the morphodynamic response of human-altered tidal embayments. *Geomorphology*, *320*, 127–141. https://doi.org/10.1016/j.geomorph.2018.08.014Zecchin, M., Baradello, L., Brancolini, G., Donda, F., Rizzetto, F., & Tosi, L. (2008). Sequence stratigraphy based on high-resolution seismic profiles in the late Pleistocene and Holocene deposits of the Venice area. *Marine Geology*, *253*(3–4), 185–198. https://doi.org/http://dx.doi.org/10.1016/j.margeo.2008.05.010Zhou, Z., Coco, G., Jiménez, M., Olabarrieta, M., Van Der Wegen, M., & Townend, I. (2014). Morphodynamics of river-influenced back-barrier tidal basins: The role of landscape and hydrodynamic settings. *Water Resources Research*, *50*(12), 9514–9535. https://doi.org/https://doi.org/10.1002/2014WR015891Zhou, Z., Chen, L., Townend, I., Coco, G., Friedrichs, C. T., & Zhang, C. (2018). Revisiting the Relationship between Tidal Asymmetry and Basin Morphology: A Comparison between 1D and 2D Models. *Journal of Coastal Research*. https://doi.org/10.2112/si85-031.1